

Impact of DEM-derived factors and analytical hierarchy process on landslide susceptibility mapping in the region of Rożnów Lake, Poland

Kamila Pawluszek¹  · Andrzej Borkowski¹

Received: 17 May 2016 / Accepted: 2 December 2016 / Published online: 27 December 2016
© The Author(s) 2016. This article is published with open access at Springerlink.com

Abstract Choosing appropriate landslide-controlling factors (LCFs) in landslide susceptibility mapping (LSM) is a challenging task and depends on the nature of terrain and expert knowledge and experience. Nowadays, it is very common to use digital elevation model (DEM) and DEM-derivatives, as a representation of the topographic conditions. The objective of this study is to explore topography in depth and simultaneously reduce redundant information within DEM-derivatives using principal component analysis. Moreover, this study investigates the impact of DEM-derived factors on LSM. Therefore, three various strategies were tested. The first strategy included a set of LCFs created from the four initial principal components, which were provided from DEM-derived factors. The second strategy included a set of parameters which contained additional lithological and environmental factors. The third strategy utilises the analytical hierarchy process (AHP) to assign weights to each LCF. The LSM was performed based on landslide susceptibility index. Obtained results show that 60% of existing landslides fell into high and very high susceptibility zones using first and second strategies. It proves that topographic factors play a significant role in LSM. Adding additional lithological and environmental factors to the set of LCFs did not improve the results significantly, unless the AHP was used in the third strategy. It improved results significantly; up to 70%. Results from second and third strategies highlight utility of AHP in LSM. Presented studies were performed on the area very prone to landslide occurrence in the region of Rożnów Lake, Poland.

Keywords Landslide susceptibility mapping · Landslide-conditioning factors · Principal component analysis · Analytical hierarchy process

✉ Kamila Pawluszek
kamila.pawluszek@igig.up.wroc.pl

¹ Institute of Geodesy and Geoinformatics, Wrocław University of Environmental and Life Sciences, Grunwaldzka 53, 50-357 Wrocław, Poland

1 Introduction

Landslides are generally defined as unexpected movements of soil, rock and organic material under the effect of gravity (Highland and Bobrowsky 2008). Landslides are a natural hazard that cause damage to the environment in many areas of the world. The slope failures can be fatal and also can destroy or damage residential and industrial facilities, as well as agricultural and forest areas. Moreover, landslides have negative effects on the quality of water in rivers and streams (Schuster and Fleming 1986). For the theory of landslide and additional background information, the reader is referred to the literature, e.g. Highland and Bobrowsky (2008). Considering landslide impact on development and urbanisation, effective landslide assessment is required (Aleotti and Chowdhury 1999). The increasing awareness of the socio-economic significance of landslides provides motivation to develop appropriate landslide risk zonation (Aleotti and Chowdhury 1999).

The first step for hazard and risk prediction is landslide susceptibility mapping (LSM). LSM is the evaluation of the ground's proneness to landslides and the possibility that landslide might occur at a specific terrain or under the influence of certain factors (Pourghasemi et al. 2013). It shows the spatial distribution of landslide-prone areas, usually as landslide occurrence probabilities distributed across grid cells (Goetz et al. 2015). Different methods of LSM have been broadly examined and analysed in the past decades (Mohammady et al. 2012; Goetz et al. 2015; Bai et al. 2010; Mashari et al. 2012; Tien Bui et al. 2011, Feizizadeh et al. 2014; Dimri et al. 2007; Kanungo et al. 2008). Moreover, numerous comparisons of LSM methods have been evaluated and still no single best method has been selected (Goetz et al. 2015). In general, methods of LSM may be qualitative or quantitative (Aleotti and Chowdhury 1999). Qualitative approaches are entirely based on the perception and experience of the person or persons who carry out the susceptibility assessment. The quantitative methods are considered as more objective than qualitative approaches due to their data-dependent characteristic. These methods cover a broad spectrum of geotechnical engineering approaches, statistical approaches, artificial neural network or fuzzy logic methods (Aleotti and Chowdhury 1999). Statistical approaches applied for modelling of the landslide susceptibility are based on the assumption that factors which caused landslides in the past are the same or similar as those which will create landslide in the future (Guzzetti et al. 1999). Therefore, these approaches concentrate on relations between landslide-controlling parameters and the location of existing landslides from landslide inventory map (Saadatkhah et al. 2014; Aleotti and Chowdhury 1999). Within statistical approaches, there are either bivariate or multi-variate analyses (Chalkias et al. 2014). Using bivariate statistical analyses, each of factors is individually compared to the landslide inventory map. These techniques apply primary-level weights, which are commonly based on certain rules. The widely used rule is landslide density, which is calculated as relation between the area affected by landslide pixels on a class of a specific factor and the total area of that class; expressed as a percentage (Ayalew et al. 2004; Akgun et al. 2008). The most frequently used bivariate methods are frequency ratio calculation, also called the landslide susceptibility index, probabilistic likelihood ratio (PLR), weight of evidence and statistical index (Kavzoglu et al. 2015a, b; Thiery et al. 2007; Mezughi et al. 2011; Yalcin et al. 2011; Abay and Barbieri 2012; Constantin et al. 2011). Among multi-variate methods, logistic regression is widely applied (Bai et al. 2010; Mashari et al. 2012). The comparison of bivariate (statistical index) and multi-variate (logistic regression) methods was performed by Tien Bui

et al. (2011). This comparison indicates an almost equal predicting capacity between these two methods.

The major difficulties in quantitative methods mentioned above are the assessment of the factors related to landslide occurrence and the assignment of appropriate weights to these factors (Carrara 1988; Bui et al. 2016; Kavzoglu et al. 2015a, b). Hence, many researchers tested different approaches, which analyse the spatial distribution of landslides with different LCFs (Bui et al. 2016; Mahalingam et al. 2016). Nowadays, the significance of each LCF can be easily validated using geographic information system (GIS). In addition, GIS provides a powerful tool for multi-criteria decision analysis (GIS-MCDA) which became more popular over the past years (Ahmed 2015; Aleotti and Chowdhury 1999). The concept of MCDA assumes that each LCF can be combined by applying primary- and secondary-level weights. Primary-level weights follow the same rule as bivariate approaches. However, secondary-level weights are expert opinion-based weights (Ayalew et al. 2004; Ahmed 2015). Among expert opinion methods for weights assignment, an analytic hierarchy process (AHP) is a technique which has been successfully applied to many decision maker systems (Kayastha et al. 2013; Ayalew et al. 2005). The AHP technique uses a pair-wise relative comparison between each LCF (Saaty 1980). Due to this fact, the weights assignment is getting more complicated and time-consuming if the quantity of LCF increases. Except for statistical methods, data mining using fuzzy logic (Feizizadeh et al. 2014; Dimri et al. 2007; Kanungo et al. 2008) and artificial neural network models (Ermini et al. 2005; Lee and Evangelista 2006; Kanungo et al. 2006) have also been applied to the LSM using GIS. Furthermore, applications of data mining and soft computing methods are increasing rapidly. Among these approaches also decisions trees, Bayesian networks, etc., are characterised by effectiveness in LSM (Bui et al. 2016).

Various natural and man-made factors can be considered as the LCFs. For that reason, the selection of the appropriate LCFs is a challenging task. LSM requires that topographic, environmental, geological and hydrological parameters should be taken into account. Some researchers assume that the accuracy of the created susceptibility map increases proportionally with the quantity of LCFs used (Jebur et al. 2014). Other scientists state that a small number of LCFs is satisfactory to produce landslide susceptibility maps with a reasonable quality (Jebur et al. 2014; Mahalingam et al. 2016). The investigations of Kingsbury et al. (1992) present that the additional factors (soil type, land use, slope aspect, proximity to watercourses) did not increase the reliability of the susceptibility maps and are suitable to a particular study area only. Therefore, no specific rule exists to define how many conditioning factors are sufficient for the susceptibility analysis on a given study area (Pourghasemi et al. 2013; Mahalingam et al. 2016). Moreover, various factors have a different impact on landslide occurrence; therefore, MCDA provides the possibility to include expert opinion to describe their impact.

The objectives of this study were to:

1. deeply explore topographic information delivered from DEM by calculating ten different DEM-derived LCFs,
2. reduce redundant information within DEM-derived factors by applying PCA technique,
3. reduce the pair-wise combinations within AHP by applying PCA technique,
4. investigate the impact of DEM-derived factors and AHP technique for LSM on the study area by applying three strategies with different data set and methods,
5. produce a landslide susceptibility map at the regional scale of the study area using probabilistic likelihood ratio method (PLR).

2 Study area characteristic

The study area covers approximately 26.3 km² and is located in the central part of the Outer West Carpathians within the Ciężkowice Foothills (Starkel 1972), along the western bank of Rożnów Lake (Fig. 1). The geographic location of this catchment area is 49°43'N to 49°46'N latitude and 20°38'E to 20°43'E longitude. The altitude of the study area ranges from 235 m to 486 m. This area was chosen because of the frequency of landslides over the past few years. Landslides in this area are commonly related with sedimentary rocks subjected to a primary driving force such as rainfall. Their activity is mostly attributed to the high variability of the hydrogeological conditions, controlled by fluctuation of water level in the Rożnów Lake and complex geology of the flysch-type rocks (Borkowski et al.

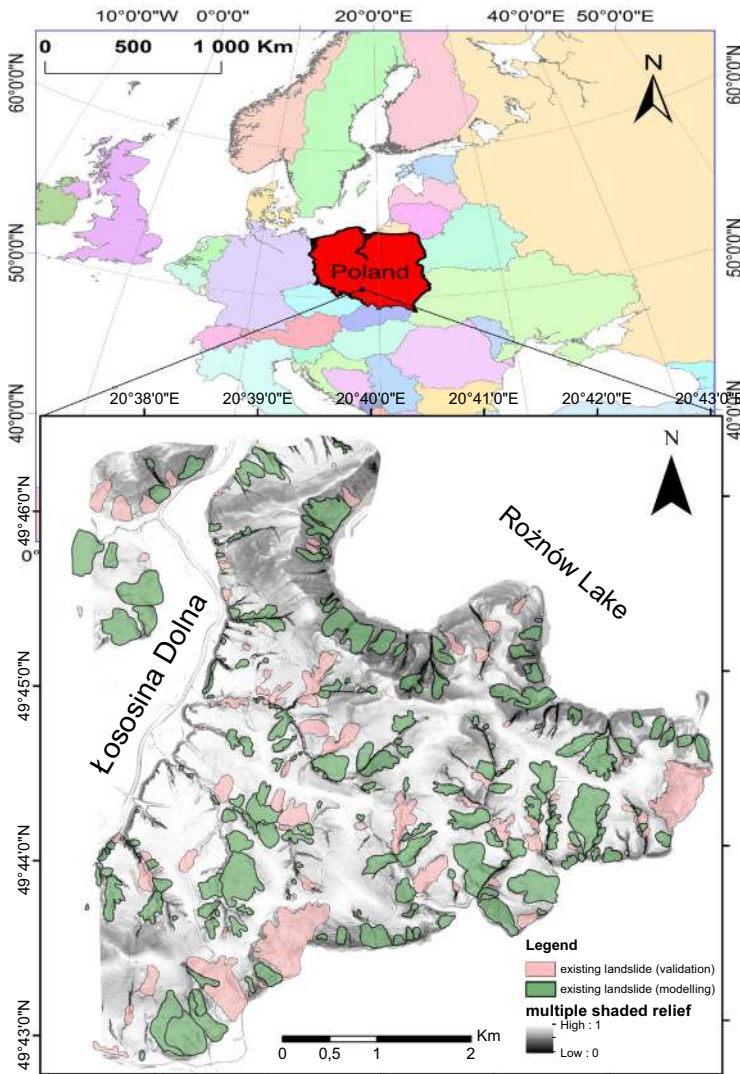


Fig. 1 Study area with landslide inventory map (landslide divided for modelling and testing data sets)

Table 1 Data used to create thematic layers

Data	Source	Type
Landslide inventory map	SOPO project	Raster
DEM	ISOK project	Point cloud
Land use and drainage maps	Topographic object database	Vector
Roads map	Open street map	Vector
Lithology map	Polish geological institute	Raster

2011). Within the study area, various landslide types can be found including: new active, suspended and dormant old. Landslides located in a forested terrain are hidden and therefore very problematic for identification. Earthflows are the main type of landslide that occurred within the study area. They usually occur on slopes above rivers and creeks. The average annual precipitation on the research area was at the level of 728.9 ± 10.7 mm in years 1981–2010 (Woźniak 2014). Most of the landslides located within the study area are: translational, rotational and combined rock-debris slides or debris slides (Gorczyca et al. 2013).

3 Data used

Due to format and data type inconsistency between the above sources, all input data were pre-processed using the ArcGIS software to create thematic layers in the raster format with pixel size $5 \text{ m} \times 5 \text{ m}$ (Pawłuszek and Borkowski 2016). These layers represent LCFs. The characteristic of the prepared layers is given below in more detail (Table 1).

3.1 Landslide inventory map

Due to the problem related to landslide occurrences and activities, Polish Geological Institute created a “Landslide Counteracting System” called SOPO (Borkowski et al. 2011). The aim of this system is to collect landslide inventory maps of all existing landslides in Poland and put them into one database. This database stores information about active, inactive and landslide-prone areas. The online database content is available to the public to browse and is free of charge. The SOPO database showed more than 250 landslides for the study area. The landslide-affected areas cover 6.51 km^2 , which means that 25% of total area is affected by landslides. It proves that the study area is very susceptible to the landslide activity and needs efficient landslide susceptibility assessment. Therefore, for modelling, 70% of randomly selected landslides was used and 30% was used for validation.

3.2 DEM-derived LCFs

All DEM-delivered layers are in GRID format with the cell size equal to $5 \text{ m} \times 5 \text{ m}$ that was generated from point cloud with resolution of 4–6 points/m². Point cloud was obtained from airborne laser scanning in the framework of the ISOK project (Pawłuszek et al. 2014). According to Pawłuszek et al. (2014), the height component accuracy of the ISOK data does not exceed 23 cm for forested areas. Based on the DEM, the presented above,

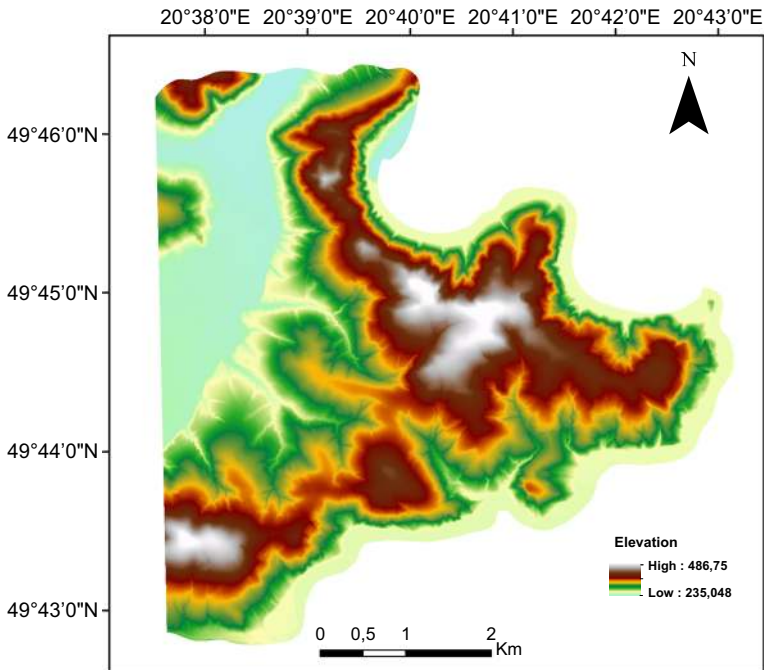


Fig. 2 Elevation

geomorphological and hydrological thematic data layers were computed. Since the most-used LCFs are commonly known, we omitted background relations needed to calculate them. We provided equations below only for new and rarely used LCFs.

3.2.1 Elevation

Many approaches for landslide susceptibility mapping consider the elevation (Fig. 2) as one of the major LCFs. There exists a close connection between elevation and landslide occurrence (Bai et al. 2010; Chen et al. 2013; Ayalew et al. 2005; Goetz et al. 2015; Chalkias et al. 2014; Jebur et al. 2014; Mashari et al. 2012; Pourghasemi et al. 2012). All DEM-delivered LCFs are calculated based on the elevation which means that they can be represented by the elevation. Ayalew et al. (2005) use the elevation as one of the only three conditioning factors for LSM.

3.2.2 Slope

The slope (Fig. 3) is the crucial landslide-conditioning factor because sliding of loose material is directly related to the slope (Bai et al. 2010; Chen et al. 2013; Ayalew et al. 2005; Goetz et al. 2015; Chalkias et al. 2014; Jebur et al. 2014; Mashari et al. 2012; Pourghasemi et al. 2012; Akgun et al. 2008; Constantin et al. 2011; Thiery et al. 2007; Sarkar and Kanungo 2004; Feizizadeh et al. 2014; Kayastha et al. 2013; Ozturk et al. 2016).

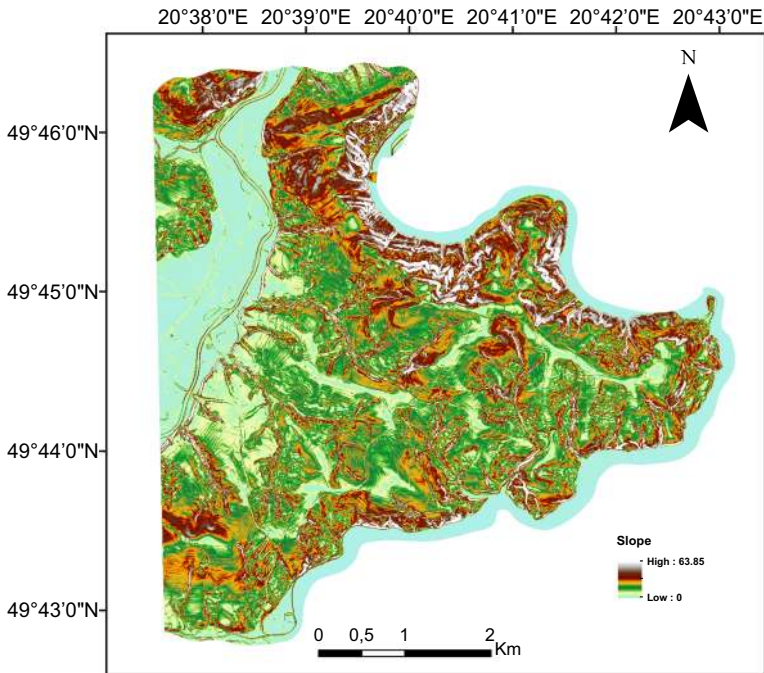


Fig. 3 Slope

3.2.3 Morphological gradient

The morphological gradient is widely used in image processing as edge detector in segmentation application, thresholding in the watershed transformation. It is characterised by difference between extensive and anti-extensive transformations (Rivest et al. 1992). Gradient operators enhance the high grey level variations. In the literature, there are different ways of morphological gradient calculation (Soille 2013). However, Beucher gradient (Fig. 4) is widely calculated as the difference between the dilation and the erosion of the image (Soille 2013). In this case, the image was created from DEM, where intensities of image pixels were calculated as the standardised elevations of the appropriate GRID cells. The morphological gradient detects the contrast intensity in the close neighbourhood of specific pixel. Thus, the morphological gradient exposes big variations of the terrain elevations. Obviously, areas with high elevation differences have a crucial influence on landslide occurrences. The morphological gradient has never been applied before in landslides studies and is introduced by the authors in this research in order to deeply explore the DEM. It is calculated for 3×3 pixel mask using plug-in implemented in Python.

3.2.4 Aspect

The aspect (Fig. 5) shows the horizontal direction of a surface. The aspect value of the slope is constant. In order to illustrate the trend of the slope, the aspect is classified into eight classes corresponding to eight geographic directions and an additional class for the flat ground. The relation between aspect and landslide occurrence has been widely

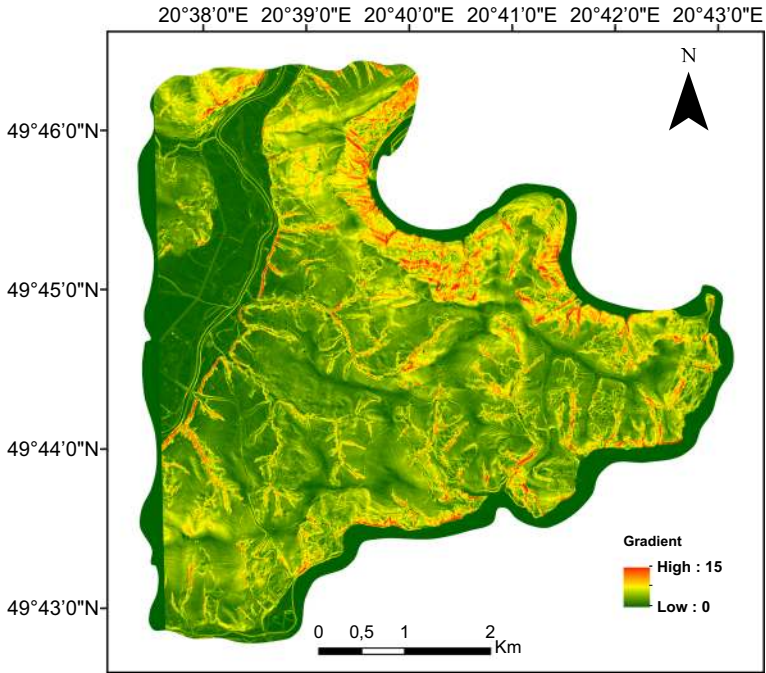


Fig. 4 Gradient

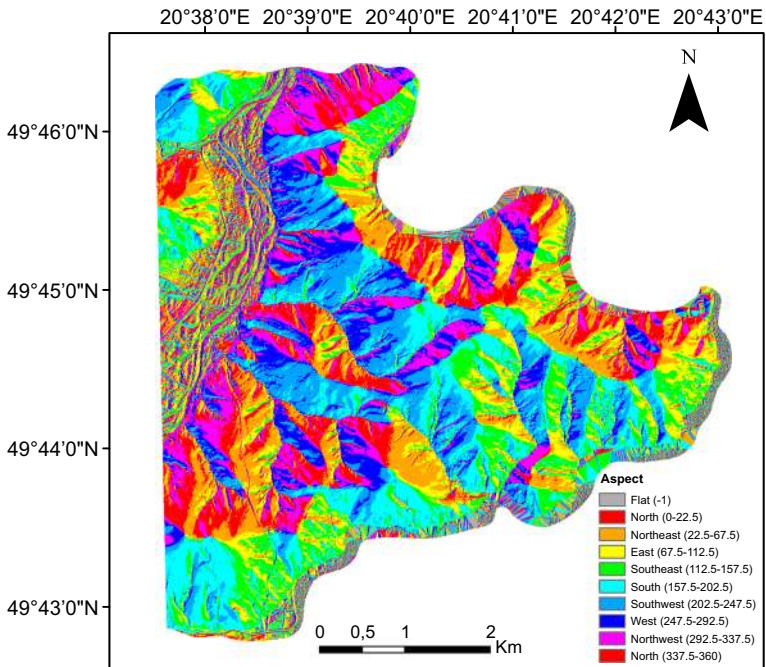


Fig. 5 Aspect

investigated for several years (Bai et al. 2010; Chen et al. 2013; Ayalew et al. 2005; Chalkias et al. 2014; Jebur et al. 2014; Mashari et al. 2012; Pourghasemi et al. 2012; Akgun et al. 2008; Constantin et al. 2011; Sarkar and Kanungo 2004; Kayastha et al. 2013). However, no clear agreement exists in the context of the aspect as a LCF. Nevertheless, the aspect was taken into account as one of the factors in this study.

3.2.5 Area solar radiation (ASR)

The area solar radiation (Fig. 6) is one of the secondary terrain derivatives and is computed based on the aspect and the slope. ASR represents the radiant energy within a given location (pixel) for the specific date. ASR combines two insolation factors: the sun angle (slope dependence) and its direction (aspect dependence). If the soil receives little amount of solar radiation, it can cause high soil moisture. It is obvious that soil with high moisture content is more prone to landslide occurrence. Moreover, higher solar radiation contributes to better vegetation growth, consequently leading to a more stable slope (Hengl and Reuter 2009; Wilson and Gallant 2000). The ASR computation is time-consuming. This may be the reason, why this factor is excluded from previous investigations unless it is easily available in ArcGIS.

3.2.6 Roughness

The roughness index (Fig. 7) is derived from the slope map by applying a moving standard deviation filter with 3x3 pixel kernel size. The roughness index is widely used in landslide

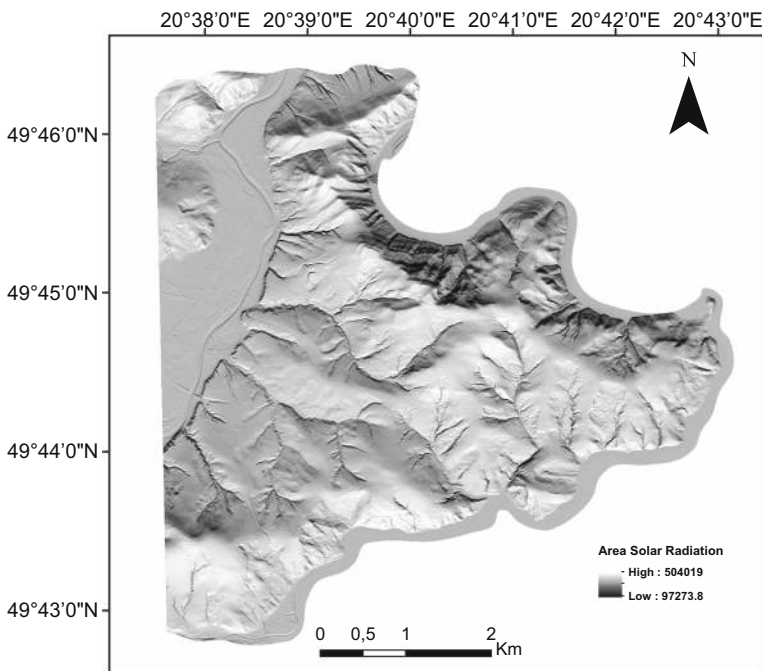


Fig. 6 Area solar radiation

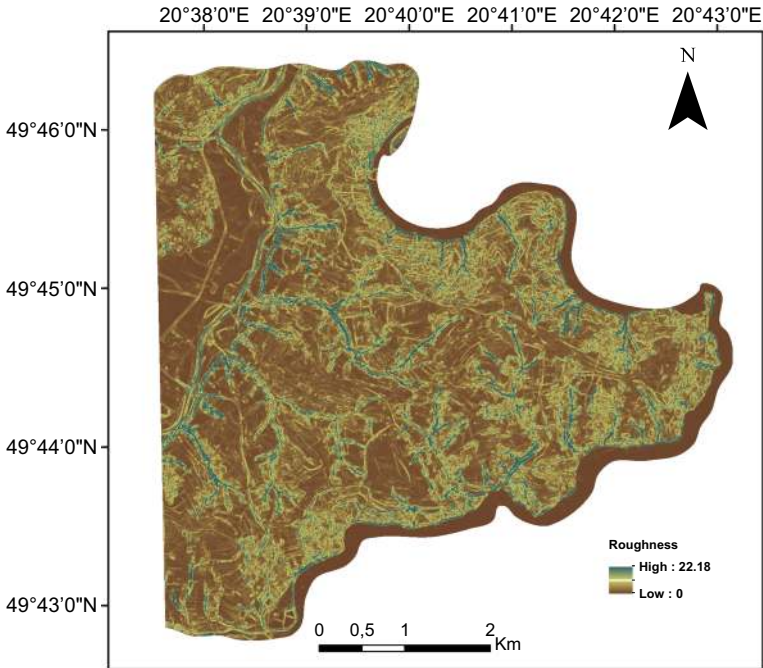


Fig. 7 Roughness

studies—in particular to create landslide inventory maps (McKean and Roering 2004). Typically, areas affected by landslides are very rough. Moreover, different roughness indexes can represent various landslide activities (Glenn et al. 2006).

3.2.7 Topographic position index (TPI)

The TPI (Fig. 8) is calculated as the difference between the cell elevation and the mean elevation of neighbouring cells. Applying specific thresholds for TPI values allows for the identification of different topographic landforms, such as ridge, slope, valley. Since the landslide scarps occur mostly on the ridges, the TPI index may be seen as one of geomorphological LCFs (Jebur et al. 2014; Pourghasemi et al. 2014). In this study, TPI was calculated using Jenness et al. (2011) implementation.

3.2.8 Topographic wetness index (TWI)

The TWI (Fig. 9) is a hydrological factor, which is widely used in landslide studies (Pourghasemi et al. 2012, 2013). This factor is applied to quantify topographic control on hydrological processes (Jebur et al. 2014; Pourghasemi et al. 2012, 2013; Akgun et al. 2008). The TWI is a function of the slope β and the upstream contributing area per unit width orthogonal to the flow direction A_s (Gessler et al. 1995; Moore et al. 1993) and is calculated as follows:

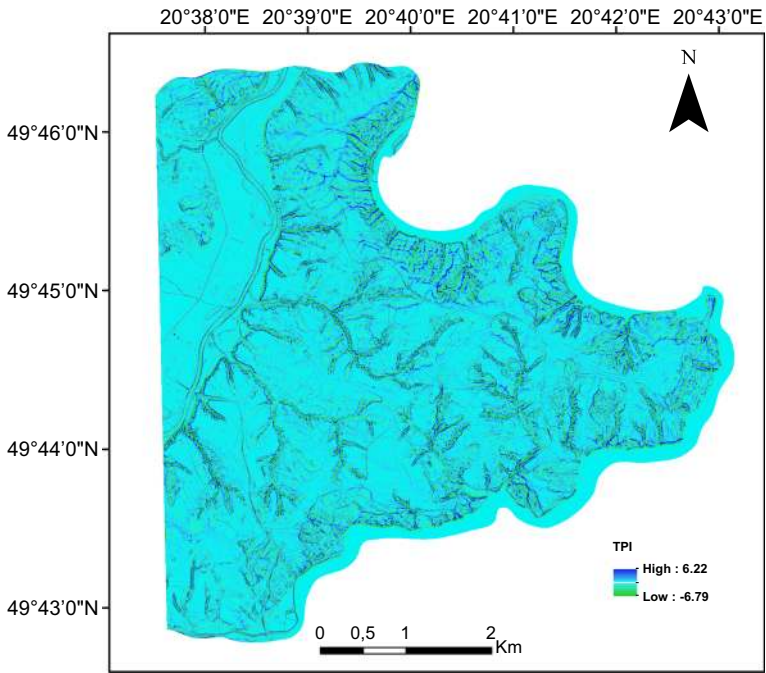


Fig. 8 Topographic position index

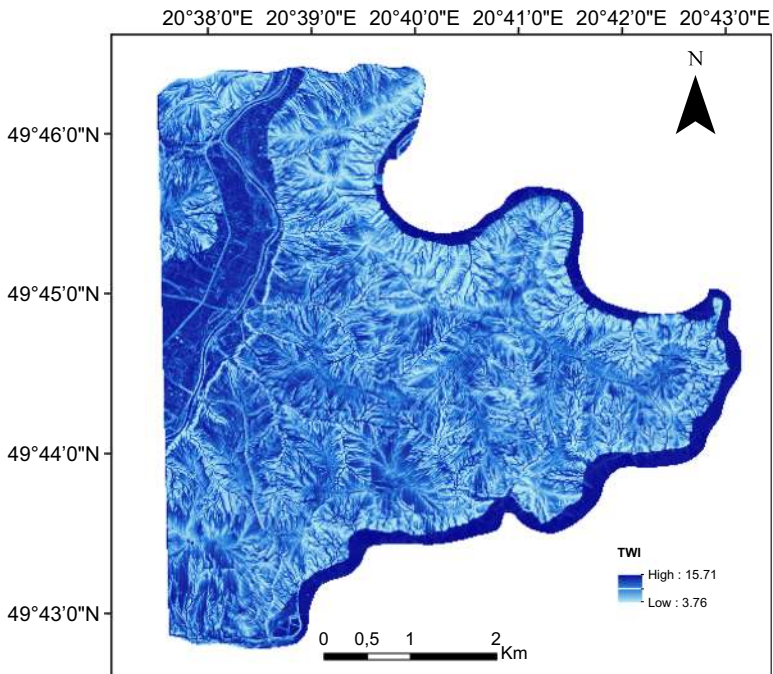


Fig. 9 Topographic wetness index

$$TWI = \ln \frac{A_s}{\tan \beta} \quad (1)$$

where A_s is area value calculated as $(\text{flow accumulation} + 1) \cdot (\text{pixel area in m}^2)$ and β is the slope (in $^\circ$).

TWI index was calculated using script from Geomorphometry and Gradient metrics written by Jeffrey Evans, which is applicable in ArcGIS (Evans et al. 2014).

3.2.9 Stream power index (SPI)

Usually, SPI (Fig. 10) is used in the landslide susceptibility studies as the meaningful hydrological factor (Pourghasemi et al. 2012, 2013; Akgun et al. 2008; Mohammady et al. 2012). However, other investigations (Gokceoglu et al. 2005) treat SPI (Fig. 2h) as a secondary important characteristic. The SPI describes potential for flow erosion at the given point of the surface, and controls potential erosive power of water flow (Moore et al. 1991). The SPI used the same variables as TWI but is calculated in different manner:

$$SPI = A_s \cdot \tan \beta \quad (2)$$

3.2.10 Shaded relief

The shaded relief (Fig. 11) describes a hypothetical illumination value of the surface. It enhances the visualisation of a surface. In presented work, multiple shaded reliefs were obtained by illuminating the DEM from eight different sun directions. Similar approach

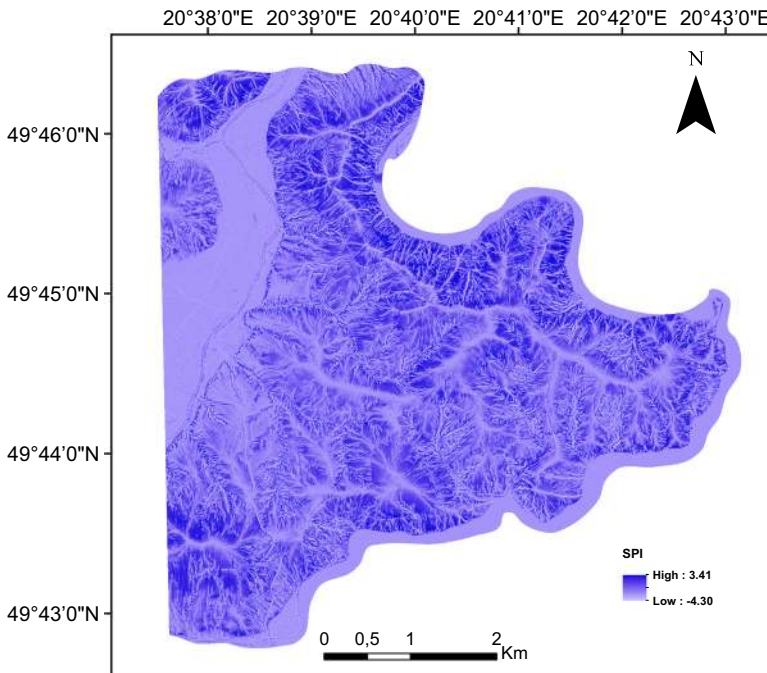


Fig. 10 Stream power index

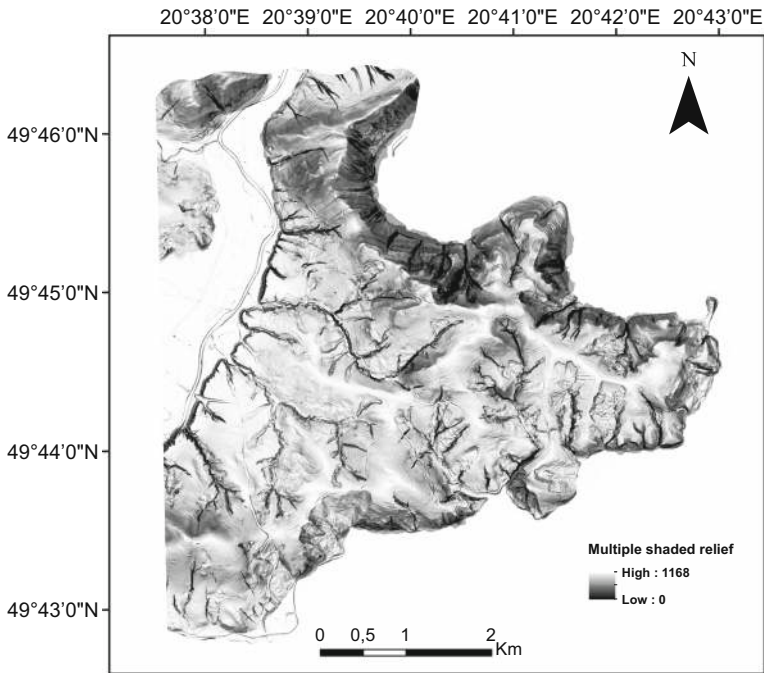


Fig. 11 Multiple shaded relief

can be found in works of Schulz (2004) and Van den Eeckhaut et al. (2007). The multiple shaded relief images are widely applied to explore deeply the morphometric information provided by DEM (Guzzetti et al. 2012).

3.3 Lithology

In some studies, the lithology (Fig. 12) is one of the essential conditioning factors in LSM (Jebur et al. 2014; Mashari et al. 2012). On the study area, eight lithological units can be distinguished that consist of: sandstone, claystone, marl and conglomerates (K2); sandstone and shales (E1); sandstone, shales, conglomerates, marl claystone and mudstone subordinate (E2); landslide deposits (Q3); sandstone, shales, schists and cornea (E3); sandstones, shales, conglomerates, marl, claystone, and sands, gravels, alluvial soils and peats, and silts (Q2); less (Q1). Appendix shows landslide percentage in each lithological unit.

3.4 Environmental factors

3.4.1 Distance from roads

Many researchers claim that the presence of roads in mountainous areas increases the chance of landslide subsistence (Akgun et al. 2008; Feizizadeh et al. 2014; Pourghasemi et al. 2012, 2013; Jebur et al. 2014; Mashari et al. 2012; Mohammady et al. 2012). Moreover, road constructions may undercut the slopes and break the rock structures, consequently decreasing the slope strengths. Therefore, the distance (Fig. 13) from roads

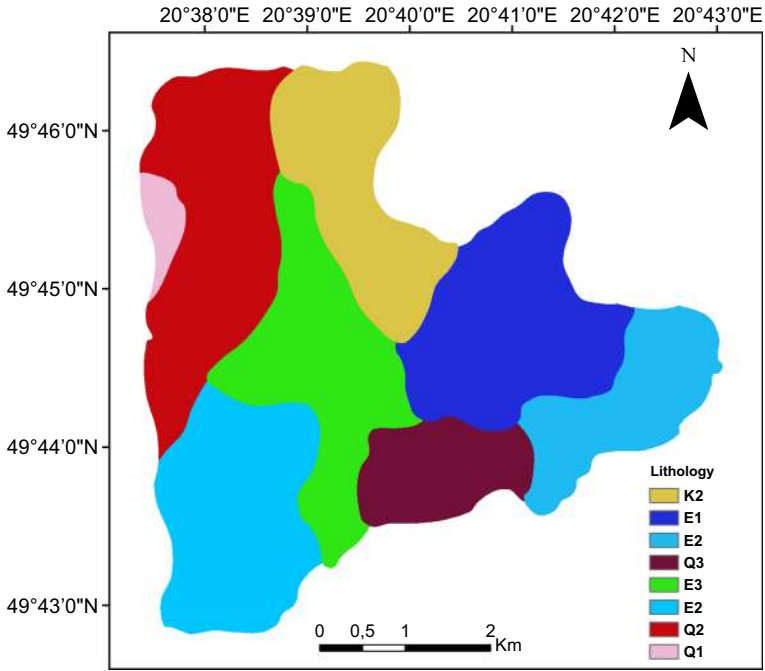


Fig. 12 Lithology

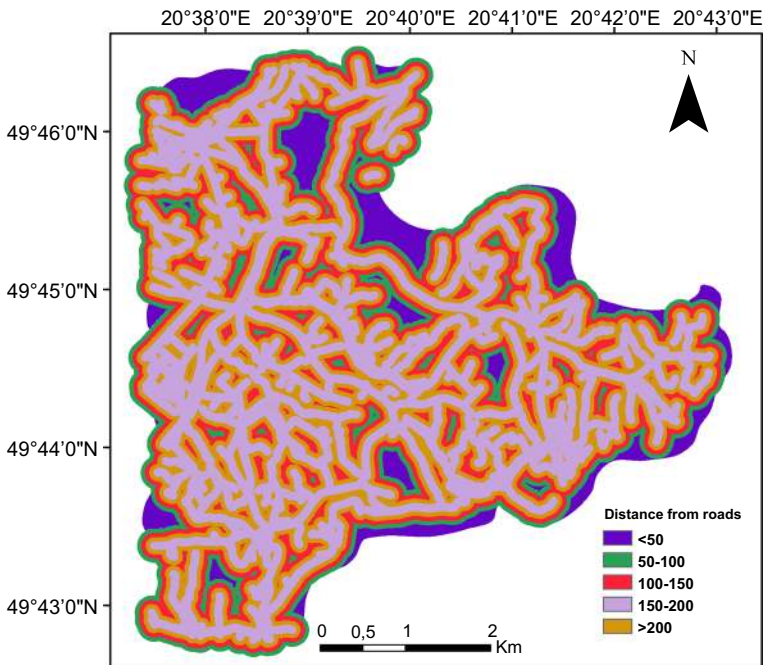


Fig. 13 Distance from roads

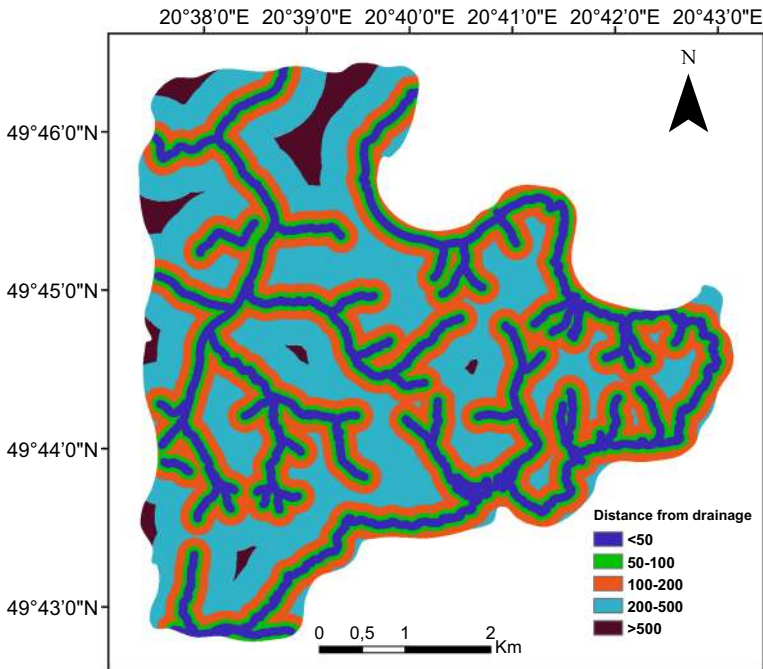


Fig. 14 Distance from drainage

(Fig. 13) is used as one of LCFs (Donati and Turrini 2002). Appendix presents the landslide density in each distance to roads category.

3.4.2 Distance from drainage

The water level fluctuation in the Rożnów Lake area is one of the crucial factors. Landslides very often occur along the riverbanks within the study area. The use of distance from drainage (Fig. 14) as the landslide-conditioning factor can be seen in many studies (Akgun et al. 2008; Chen et al. 2013; Sarkar and Kanungo, 2004; Feizizadeh et al. 2014; Pourghasemi et al. 2012, 2013; Jebur et al. 2014; Mohammady et al. 2012). Hence, this factor should be considered as one of LCFs. Appendix shows the landslide density as the percentages in every distance interval from the drainage class. It is evident that landslides occur mainly at the distances less than 100 m.

3.4.3 Land use

The land use (Fig. 15) demonstrates how people use the landscape whether for development, conservation or mixed uses. It is obvious that different land use has different impact for slope stability. Therefore, land use is an essential factor in LSM in many studies (Chen et al. 2013; Constantin et al. 2011; Sarkar and Kanungo 2004; Kayastha et al. 2013; Kanungo et al. 2006; Pourghasemi et al. 2012, 2013; Mashari et al. 2012; Mohammady et al. 2012). Bare slopes are more susceptible to landslide occurrence (Van Westen et al. 2008). Land use changes caused by human activities, such as cultivation or deforestation, may have a significant impact on the landslide activity (Van Westen et al. 2008). However,

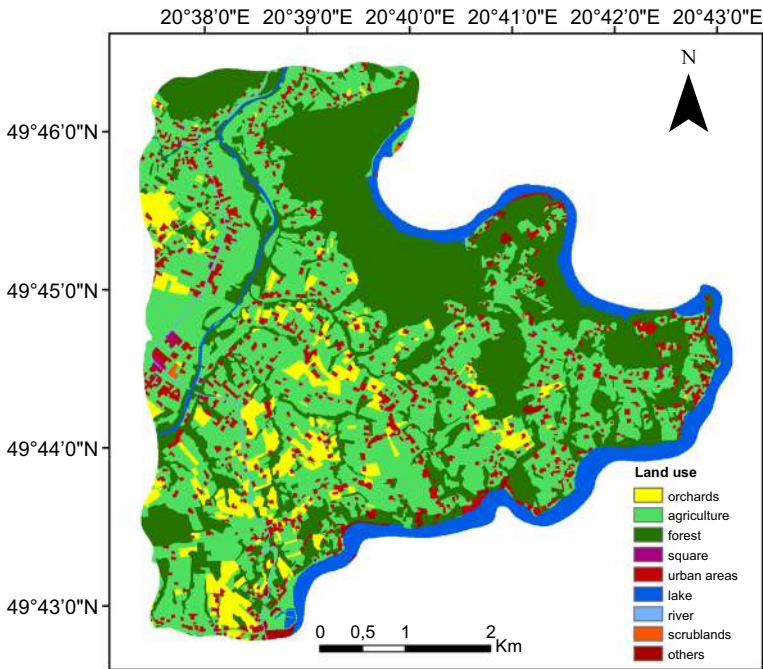


Fig. 15 Land use

vegetative areas tend to prevent the erosion and decrease the landslide susceptibility because of the natural anchorage constructed by the roots (Dahal et al. 2008). Appendix presents the landslides density as the percentages in every land use category. It is easy to see that landslides mostly occur in orchards and forests.

4 Methods

In order to describe the influence of DEM-derived and environmental factors on LSM, three different strategies were tested in this study (Table 2). The first strategy uses only the DEM-derived conditioning factors. The second strategy uses the full set of the LCFs that includes geological and environmental factors. Each LCF was treated equally in first and second strategies. The third strategy applies the AHP method in order to assign weights to all described LCFs and to produce the landslide susceptibility map for the study area. The

Table 2 Differences between strategies applied for LSM

	First strategy	Second strategy	Third strategy
Data used	4 principal components	4 principal component, lithology, distance do drainage, distance to roads, land use	4 principal component, lithology, distance do drainage, distance to roads, land use
Method	Probabilistic likelihood ratio (PLR)	Probabilistic likelihood ratio (PLR)	Multi-criteria decision analysis (PLR + AHP)

methodology flow chart is presented in Fig. 16 and commented in the following subsections.

4.1 Reduction of DEM-derived landslide-conditioning factors

As mentioned earlier, no universal guidelines exist for selecting appropriate factors that affect landslides and can be used in the susceptibility mapping. Moreover, an excessive number of LCFs significantly extends computational time. Nevertheless, in the presented approach abundant topographic LCFs were considered. As mentioned previously, quantitative approaches demand weights to be assigned to each LCF. Hence, many researchers use AHP to determine weights for landslide-controlling factors. This method requires pairwise comparisons of each LCF. The AHP is subjective approach, because it is based on the knowledge and an expert opinion. Moreover, if the number of used factors is bigger than the weights assigning process is the more complex. On the other hand, the selection of causal factors reflects the nature of the research area and has a certain degree of affinity with landslides (Ayalew et al. 2005). Since the DEM-delivered factors are the first or second order derivatives of the DEM, they contain redundant information. For that reason, it is rational to reduce such information. In order to extract as much information as possible from the DEM-derived factors presented above and simultaneously reduce the number of components used, the PCA was applied.

The PCA is a multi-variate approach that uses data sets, where observations are characterised by several inter-correlated quantitative dependent variables. Its objective is to extract the relevant information from the data to represent it as a set of the new orthogonal

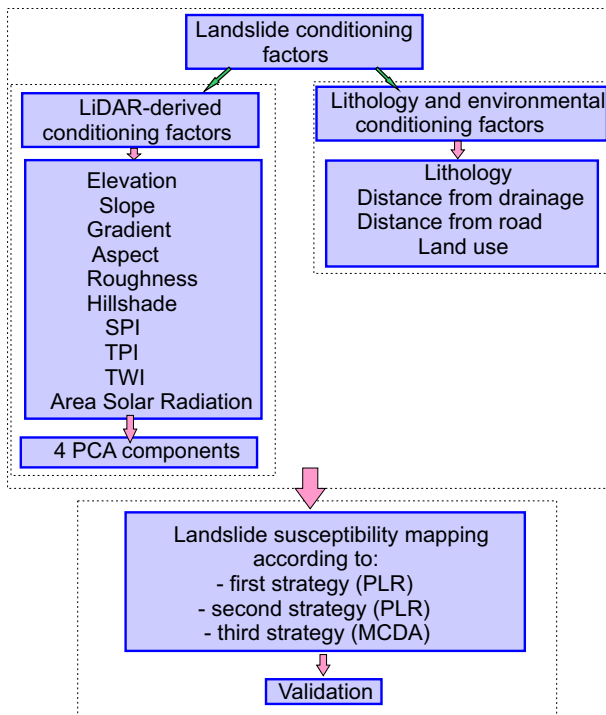


Fig. 16 Methodology flowchart

variables called principal components (Abdi and Williams 2010). Thus, normalisation of each LCF was performed before applying the PCA. According to the results, Fig. 17 shows the accumulated eigenvalues contained in the subsequent principal components. Although there are many rules which explain how many principal components should be taken into account, one is empirical criterion, where the number of principal components should include at least 80% of the total variance (Solanas Pérez et al. 2011). Analysing Fig. 17 it can be seen that the initial four principal components provide around 90% of the total variance. Therefore, in the next steps it has been decided to use only four principal components.

4.2 Calculation of probabilistic likelihood ratio (PLR)

The PLR takes advantage of the relation between existing landslides in every class (category) of each LCF. In other words, it represents landslide density and non-landslide density in each class of LCFs and it exhibits the correlation between the landslide occurrence and the LCFs in the study area (Lee and Evangelista 2006). Since the number of the DEM-derived factors was reduced to four using PCA, the PLR was calculated for the four principal components and all environmental factors (e.g. land cover, lithology). Therefore, if j is a class of LCF i , then the PLR for this class and this LCF ($PLR_{i,j}$) is determined as follows (Pourghasemi et al. 2014):

$$PRL_{i,j} = \frac{\text{No.of landslide pixels}}{\text{Total landslide pixels}} \bigg/ \frac{\text{No.of pixels in domain}}{\text{Total pixels}} \quad (3)$$

The landslide density and the non-landslide density were calculated based on the overlying landslides pixels with the thematic layers, which represent LCFs. The thematic layers were produced from environmental conditioning factors and the initial four principal components, which represent DEM-derived features. Values of landslide factors were divided into five classes using the natural breaks classification. Appendix presents the PLR in every class of the LCF. Afterwards, the PLR of each parameter class was normalised and summed and final

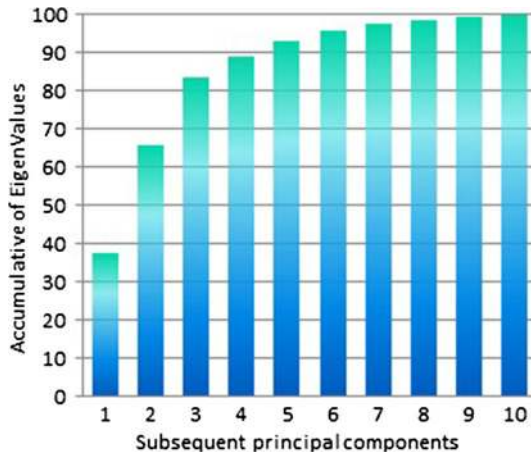


Fig. 17 Accumulative eigenvalues in subsequent principal components

susceptibility index (LSI) for each pixel was calculated using equation (Pourghasemi et al. 2014):

$$LSI = \sum_{i=1}^n PLR_{i,j} \tag{4}$$

where PLR_i is the likelihood ratio for the factor i and pixel j and n is the total number of factors.

The PLR method consists of three main steps:

- LCFs values categorisations.

In this step, the natural breaks classification was used to reclassify continuous values of four principal components into five categories. The environmental factors (such as distance to drainage or roads) were reclassified using distance buffer analysis (Chalkias et al. 2014).

- Probabilistic likelihood ratio computation according to Eq. (3)

At this stage, each class within LCF was overlaid with the landslide inventory map. Afterwards, PLR was calculated for each category by dividing the landslide density by the non-landslide density (Chalkias et al. 2014).

- Final LSI calculation for each pixel of the study area according to the Eq. (4)

At this stage, the final LSI was produced for each pixel by summing the PLR values for all LCFs computed for that pixel (Chalkias et al. 2014).

4.3 Multi-criteria decision analysis

The concept of multi-criteria decision analysis (MCDA) is that each LCF can be combined by applying primary- and secondary-level weights. Primary-level weights are received by applying PLR; however, secondary-level weights are expert opinion-based weights. For assignment of secondary-level weights, analytic hierarchy processes were applied (AHP). Therefore, the mathematical representation of MCDA is applied as follows:

$$LSI = \sum_{i=1}^n w_j \cdot PLR_{i,j} \tag{5}$$

where w_j is the weights assigned using AHP for factor j .

4.3.1 Principal component physical representation

As it was previously stated, the four initial principal components were used as a representation of DEM-derived factors. It is not easy to understand the physical meaning of each principal component and compare them. Therefore, it is desirable to find the correspondences between each principal component and DEM-derived parameters. For better understanding of principal variables, the correlation coefficients between the four principal components and ten original DEM-derived factors were computed (Table 3). The correlation is considered as strong if the absolute value of coefficient is greater than 0.5. Therefore, correlations above this value were treated as significant. Obtained coefficients show that the first component is highly correlated only with the aspect. Similarly, the component four is mostly correlated with the ASR, though the correlation with other

Table 3 Correlation coefficients between PC components and DEM-derived factors

DEM-derived factor	Principal component			
	1	2	3	4
Aspect	1.00	0.00	−0.02	−0.01
ASR	0.04	−0.20	0.48	0.79
CTI	−0.01	−0.62	0.31	−0.38
Elevation	0.02	0.84	0.53	−0.07
Gradient	−0.03	0.68	−0.62	0.03
Shaded relief	0.04	−0.58	0.66	0.04
Slope	−0.03	0.63	−0.58	0.03
SPI	0.00	0.09	0.00	−0.22
Roughness	−0.02	0.28	−0.58	0.18
TPI	0.00	0.01	0.14	0.19

factors is negligible. In the case of components two and three, the correlation with the DEM-derived factors is more complex. There is not any dominant correlation, and significant coefficients exist for more than a single factor. Both components present high correlation with the gradient, slope, shaded relief and elevation. Moreover, the component two is more correlated with CTI, while the component three is correlated with the roughness. Therefore, in the pair-wise comparison, the component two was treated mostly such as CTI and the component three mostly such as roughness.

4.3.2 Secondary-level weight assignment by AHP

The appropriate weight assignment is a challenging task. For that purpose, the AHP is used in many landslide studies in the world (Akgun et al. 2008; Kayastha et al. 2013; Ayalew et al. 2005; Feizizadeh et al. 2014). AHP is the multi-criteria decision model, which uses pair-wise comparisons of relative factors without inconsistencies in the decision process (Saaty 1980). The essential advantage of the AHP is involving the expert's knowledge and experiences in the weights assigning process. This may improve the quality of the susceptible maps. On the other hand, the AHP is subjective and different researchers can achieve different results.

In the presented study, the AHP was used to assign weights to controlling factors. The pair-wise comparison in AHP starts with assigning the preference factor to the LCFs (in this case to the four principal components and environmental factors) according to Table 4 provided by Saaty (1977). As a result of the pair-wise comparison of all LCFs, a matrix containing preference factors is created. The scale of preference factors ranging from 1 to 9 represents the direct relation between the factors, while the scale ranging from 1/2 to 1/9 means that the factors have the inverse relation (Table 5). While consensus in the pair-wise comparison is reached, weights for every vector are assigned by the eigenvector calculation using the comparison matrix. The inconsistencies in the decision process can be detected using consistency index (CI) that is defined as follows:

$$CI = \frac{\lambda_{\max} - N}{N - 1} \quad (6)$$

where λ_{\max} is the largest eigenvalue and N is the order of the comparison matrix. If CI is greater than 0.1, the comparison matrix is inconsistent and it should be revised. In the presented study, CI equal to 0.056 was obtained, which means that the comparison matrix is consistent (Saaty 2000).

Table 4 Scale of preference between two parameters in AHP (Saaty 1977)

Preference factor	Degree of preference	Explanation
1	Equally	Two factors contribute equally to the objective
3	Moderately	Experience and judgment slightly to moderately favour one factor over another
5	Strongly	Experience and judgment strongly or essentially favour one factor over another
7	Very strongly	A factor is strongly favoured over another and its dominance is showed in practice
9	Extremely	The evidence of favouring one factor over another gives the highest degree of affirmation possible.
2,4,6,8	Intermediate	Used to represent compromises between the preferences in weight 1,3,5,7 and 9
Reciprocals	Opposites	Used for inverse comparison

Table 5 Pair-wise comparison matrix and weights for landslide causative factors

LCFs (after PCA)	The first component	The second component	The third component	The fourth component	Geology	Distance from river	Distance from roads	Land use	Weights
The first component	1								0.022
The second component	9	1							0.332
The third component	7	1/2	1						0.181
The fourth component	7	1/4	1	1					0.129
Lithology	4	1/6	1/3	1/4	1				0.050
Distance from river	8	1	1/3	1	2	1			0.127
Distance from roads	4	1/5	1/2	1	2	1	1		0.089
Land use	2	1/8	1/3	1/2	2	1	1	1	0.07

Consistency index = 0.056 < 0.1 (acceptable)

4.4 Isodata classification

In order to create landslide susceptibility zones, it is necessary to reclassify the continuous values of LSI in the final map. Various classification methods are available in GIS; however, four methods, namely: standard deviations, equal intervals, natural breaks and quantile, have been examined in the landslide studies (Ayalew and Yamagishi 2005). All mentioned methods of the classification depend on the statistical parameters. Previously, clustering was not commonly used to differentiate the susceptible classes. The natural breaks classification, the quantile classification and clustering were tested in this study to divide LSI in five susceptible classes. Based on the validation method presented in Sect. 4.5, the clustering provided the best performance. In this study, the isodata unsupervised classification was used to create classes of the landslide susceptibility. The isodata were performed in ArcGIS software (Ball and Hall 1965).

4.5 Validation of landslide susceptibility maps

Remondo et al. (2003) proposed a validation method for LSM, where the original landslide inventory map is randomly split in two parts: one for the susceptibility analysis and second for validation process. According to this concept, 70% of randomly selected landslide was used for modelling and 30% was used for validation in this study.

4.5.1 SCAI index

Moreover, the seed cell area index (SCAI) validation technique proposed by Süzen and Doyuran (2004) was implemented. The SCAI is calculated by dividing percentage of pixels of the specific landslide susceptibility class by percentage of existing landslides pixels in the specific landslide susceptibility zone. SCAI shows the density of landslides among the landslide susceptibility zones. It is expected that the high and very high susceptibility classes should have very small SCAI values and low, very low susceptibility zones should have higher SCAI values (Süzen and Doyuran 2004; Kincal et al. 2009).

4.5.2 Difference image analysis

In order to compare maps from three strategies, difference image analysis was applied. Difference image analysis provides information how maps are different from each other. By comparing two landslide susceptibility maps with different susceptibility zones, the so-called residual map is received (Gupta et al. 2008). This map elucidates how pixels shift from one landslide susceptibility zone to another zone between two maps. Therefore, a residual map can have a maximum five different classes: no difference, one-zone difference, two-zone difference, three-zone difference and four-zone difference. The best performance of LSM is presented by third strategy, where AHP method was used in order to assign weights to LCF.

5 Obtained landslide susceptibility maps and discussion

The first LSM strategy used only factors derived from the DEM, which were then represented by the four uncorrelated principal components (Sect. 4.1). Landslide susceptibility maps obtained by first, second and third strategies are presented in Figs. 18, 19 and 20,

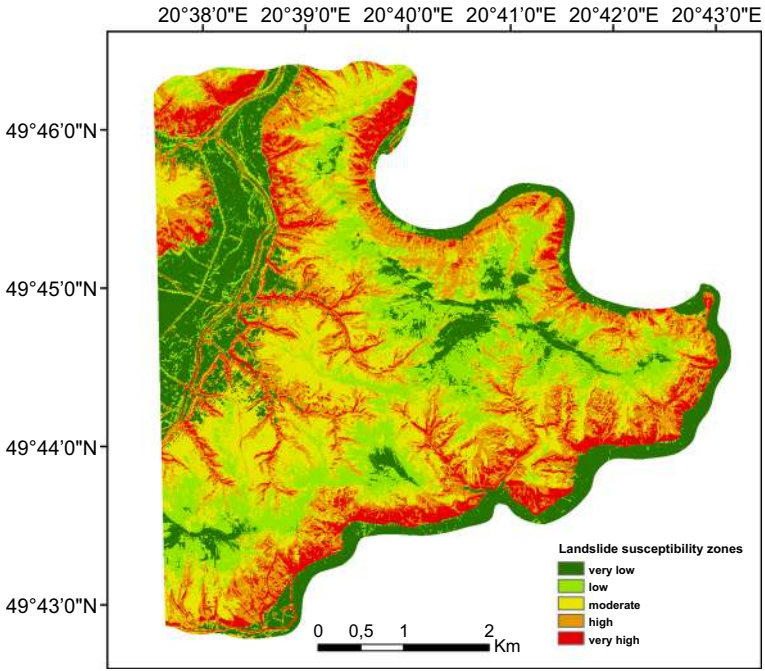


Fig. 18 Landslide susceptibility map (first strategy)

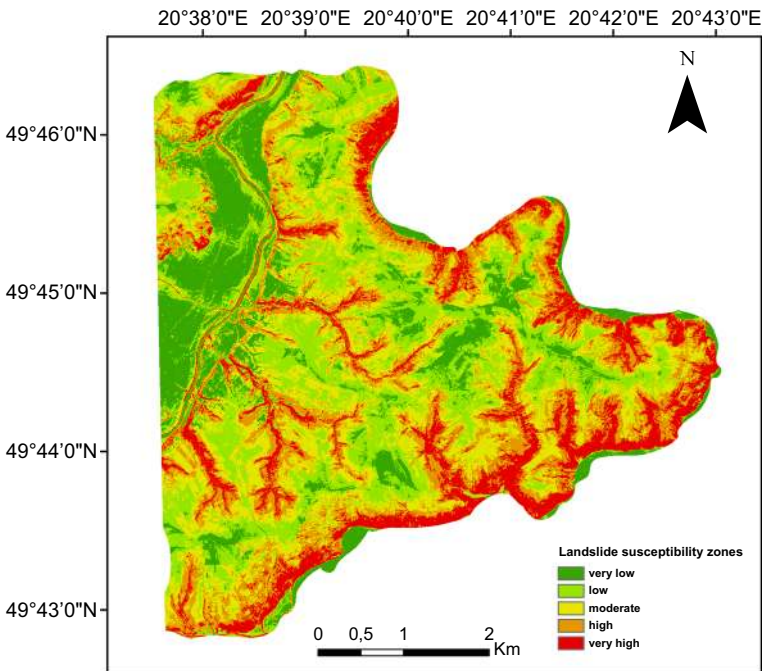


Fig. 19 Landslide susceptibility map (second strategy)

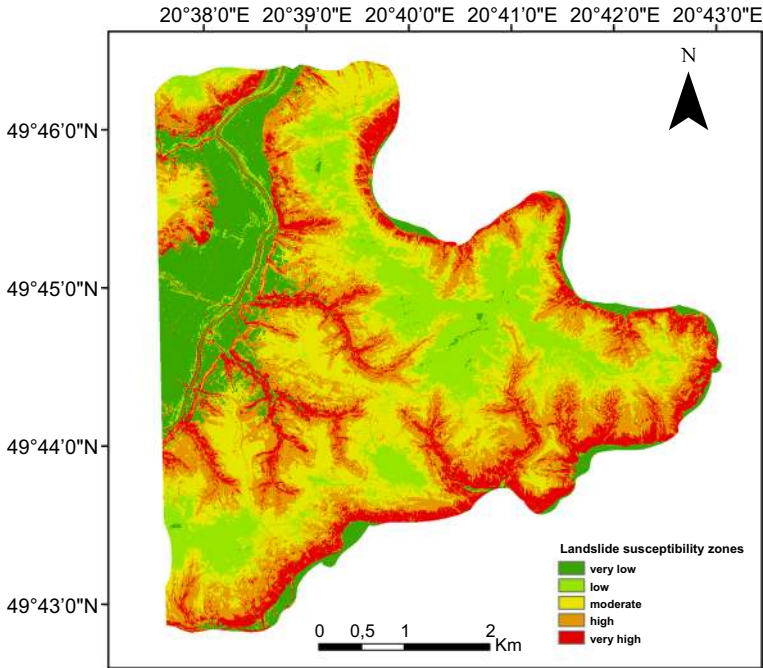


Fig. 20 Landslide susceptibility map (third strategy)

respectively. Tables 6, 7 and 8 show the percentage of landslide area in every susceptible zone and SCAI index for three strategies.

According to the first strategy, very high and high susceptibility classes contain 60% of existing landslides area used for validation. According to the second strategy, the set of parameters was extended by lithological and environmental factors. Environmental factors include distance to drainage, distance to roads and land use. Using the second strategy,

Table 6 Landslide density among the landslide susceptibility classes, the first strategy

Susceptibility	Area (%)	Seed (%)	SCAI
Very low	0.20	0.02	9.28
Low	0.20	0.09	2.25
Moderate	0.27	0.30	0.89
High	0.21	0.35	0.60
Very high	0.13	0.25	0.51

Table 7 Landslide density among the landslide susceptibility classes, the second strategy

Susceptibility	Area (%)	Seed (%)	SCAI
Very low	0.16	0.02	7.12
Low	0.25	0.10	2.40
Moderate	0.26	0.27	0.94
High	0.19	0.33	0.59
Very high	0.14	0.27	0.52

Table 8 Landslides density among the landslide susceptibility classes, the third strategy

Susceptibility	Area (%)	Seed (%)	SCAI
Very low	0.15	0.02	6.30
Low	0.17	0.06	3.04
Moderate	0.26	0.22	1.21
High	0.26	0.41	0.64
Very high	0.16	0.29	0.53

very high and high susceptibility class contains also 60% of the existing landslide area used for validation.

Comparing the results to the first strategy, it can be seen that the same percentage of landslides areas fell into high and very high susceptibility class. However, SCAI index is higher for very low and low classes for strategy using only DEM-derived factors. According to that, it can be concluded that LSM using only the four principal components obtained from DEM-derived factors provides slightly higher performance than LSM that uses all factors. It is supposed that environmental factors should increase the performance of LSM. The reason for that could be that extended set of DEM-derived factors was taken into account. For instance SPI or CTI, which are hydrological factors derived from DEM, contains information, which can be also contained in distance to drainage factor.

In third strategy-MCDA, full set of LCFs was applied with weights assigned using AHP (Sect. 4.3). The SCAI index is smaller for very low susceptible class. Very high and high susceptibility classes contain 70% of the existing landslides areas used for validation. It means that susceptibility mapping using full data set with weights exhibits the highest performance.

In order to perform difference image analysis, maps from first and second strategies were compared with the map produced in third strategy. Figures 21 and 22 present the differences in susceptible zones between these maps. Based on achieved results, it can be concluded that maps delivered using first and second approaches provide quite similar

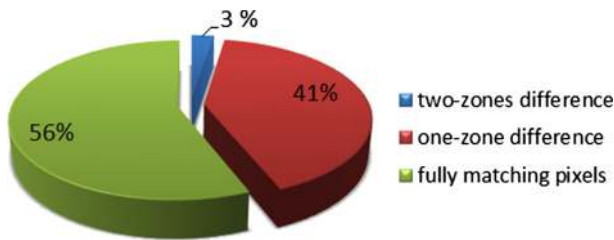


Fig. 21 Statistics for difference image analysis between first and second strategies

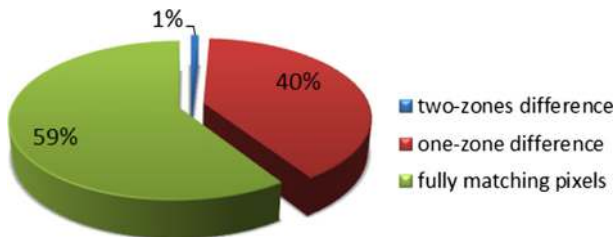


Fig. 22 Statistics for difference image analysis between second and third strategies

results in comparison with a map provided by third strategy. There is 3% of difference in number of fully matching pixels and 1% difference in one-zone difference. Between maps from strategy first and second, we can observed 59% of matching pixels (Fig. 23). Based on achieved results of compared maps, it can be stated that landslide susceptibility maps delivered only from deep exploration of DEM are not significantly worse than those created from full data set. Figures 24, 25 and 26 present residual map between first and third strategies, second and third strategies and first and second strategies, respectively. Observing residual maps (Figs. 24, 25, 26) from difference map analysis, it can be seen that the biggest difference is located close to the rivers.

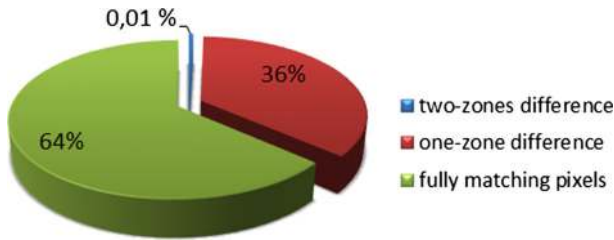


Fig. 23 Statistics for difference image analysis between first and third strategies

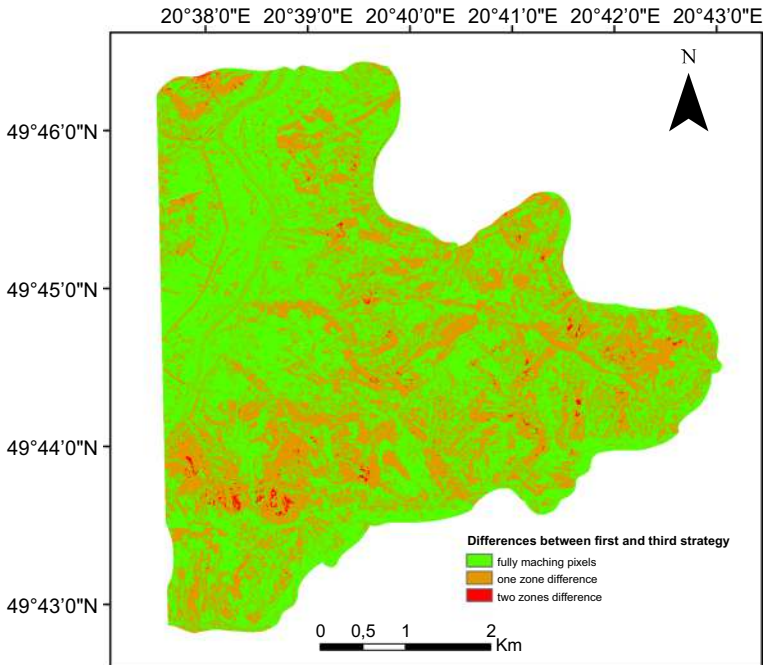


Fig. 24 Residual map between first and third strategies

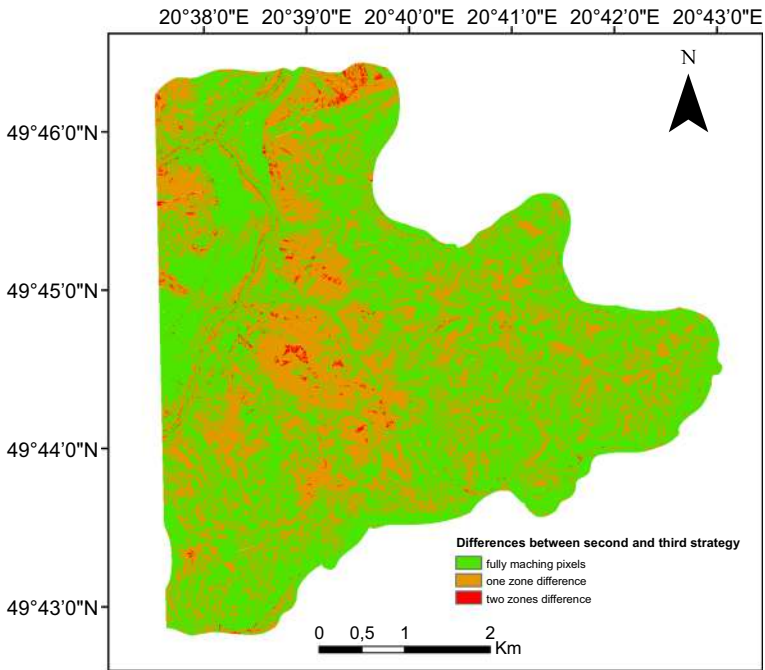


Fig. 25 Residual map between second and third strategies

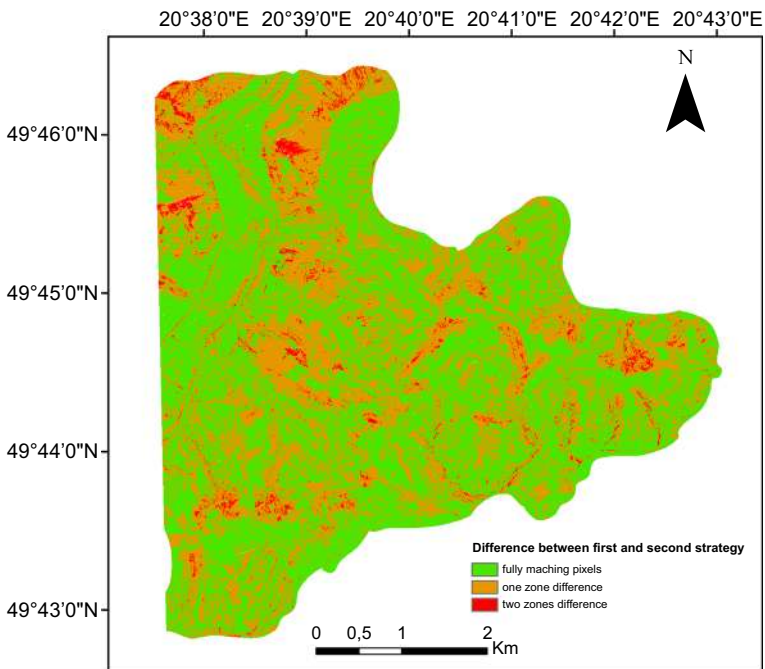


Fig. 26 Residual map between first and second strategies

6 Summary and conclusion

In presented study, three various strategies were applied to create landslide susceptibility maps for the area of Rożnów Lake, Poland. The first strategy used only DEM-derived conditioning factors reduced to four uncorrelated principal components. The second strategy used the full set of LCFs that included four principal components, lithological and environmental factors. The third strategy utilised the full set of LCFs with weights assigned using AHP. The produced susceptibility maps were compared with 30% of randomly selected landslides for validation, and the effectiveness of these three strategies was tested. Based on the achieved results, the third strategy exhibits the best performance. According to our results, the only way to achieve improved performance of LSM is to assign appropriate weights to LCFs, e.g. deploying AHP.

Besides producing the landslide susceptibility map for the study area, the main objective of this study was to investigate the impact of DEM-derived and environmental conditioning parameters for LSM in the area of Rożnów Lake. The difference image analysis between first and second strategies demonstrated the usefulness factors delivered from DEM. Comparing the SCAI, it can be concluded that LSM using only the four principal components obtained from DEM-derived factors provides slightly higher performance than LSM that uses all factors. Based on achieved results, it can be stated that landslide susceptibility maps, created using only DEM-delivered factors, provide the possibility to produce reasonable landslide susceptible zones in areas where full data collection is complicated and time-consuming. Approximately the same content of landslide areas (60%) selected for validation fell into high and very high susceptible zones in the first and the second strategies. The reason for that could be that non-DEM-delivered factors do not provide additional information, because of so deep exploring of the DEM. For instance, landslides often occur close to rivers, which can be indirectly represented by slope, roughness index or stream power index. Another reason for that could be that buffer classes of distance from drainage or roads were not chosen appropriately. It could be also that no relationship exists between landslides and land cover or lithology. It means that these LCF are not suitable to this particular study area.

After applying the AHP to assign weights to the LCFs, the effectiveness of the LSM increased up to 70%. Based on the weights assigned to the LCFs, it can be concluded that in the LSM the most important LCFs are the principal components two, three and four. They mostly correspond to the slope, elevation, roughness and ASR. Moreover, results indicated that distance to rivers is also a relevant factor in LSM. However, lithology does not have significant impact on LSM. Based on PLR obtained for each lithological class, it can be seen that the landslide occurrence in each lithological category is very similar. The reason for that could be the geological structure in the study area. Each lithological unit exhibits the same proneness for landslide occurrence. Moreover, the weights indicated that land use and aspect are not significant LCFs in LSM.

An open question is finding a proper criterion for choosing the optimal number of the principal components that represent DEM-derivatives in order to reduce the computational effort and the complexity of LSM and simultaneously to achieve a reasonable accuracy of LSM. This issue should be addressed in the future research.

Based on achieved results, this approach can be applicable to the landslide susceptibility mapping in other regions in the world. However, it is important to assign appropriate weights into the specific landslide-controlling factors, because it is mostly attributable to the nature of the terrain and type of landslide. On the other hand, most of the landslides

located within the study area have different types (translational, rotational and combined rock-debris slides or debris slides); therefore, it suggests that methodology is more comprehensive and not narrowed into one type of landslide.

Akgun et al. (2008) obtain higher performance of the LSM using the same PLR method with weights, assigned from the AHP in the study area in Turkey. On the other hand, Komac (2012) applied other bivariate Monte Carlo approach in Slovenia achieving also 70% of correctness. Similar results can be found in work (Mashari et al. 2012; Akgun and Türk 2010; Ayalew et al. 2005; Kanungo et al. 2006). According to the results, the presented approach provides diverse results for diverse study areas in the world. Moreover, choosing the most appropriate method for the LSM is essential, because it provides different results depending on the nature of the terrain. For this reason, more studies have to be performed in the Carpathian Mountains in order to select suitable methods for the LSM in this region. It will be investigated by authors in a further work. Furthermore, many other LCFs have not been tested; therefore, the authors will test importance of other LCFs on LSM, for instance distance to faults, distance to lineament, NDVI and soil depth or texture.

Open Access This article is distributed under the terms of the Creative Commons Attribution 4.0 International License (<http://creativecommons.org/licenses/by/4.0/>), which permits unrestricted use, distribution, and reproduction in any medium, provided you give appropriate credit to the original author(s) and the source, provide a link to the Creative Commons license, and indicate if changes were made.

Appendix

See Table 9.

Table 9 PLR calculation

Landslide-conditioning factors	Class	Pixels with land slides	Landslide density $\left(\frac{\text{No. of landslide pixels}}{\text{Total landslide pixels}}\right)$	Pixels with non-land slides	Non-landslide density $\left(\frac{\text{No. of pixels in domain}}{\text{Total pixels}}\right)$	$PRL_{i,j}$	Nor malised $PRL_{i,j}$
The first principal component	1	17,890	0.10	120,455	0.13	0.79	0.10
	2	22,999	0.13	116,374	0.12	1.05	0.13
	3	29,503	0.16	109,546	0.11	1.44	0.18
	4	30,954	0.17	113,627	0.12	1.45	0.18
	5	24,815	0.14	137,145	0.14	0.97	0.12
	6	18,312	0.10	122,997	0.13	0.79	0.10
	7	18,113	0.10	109,091	0.11	0.89	0.11
	8	16,355	0.09	125,294	0.13	0.70	0.09
The second principal component	1	5253	0.03	220,177	0.23	0.13	0.03
	2	59,727	0.33	206,972	0.22	1.53	0.31
	3	65,514	0.37	245,512	0.26	1.42	0.29
	4	34,235	0.19	187,687	0.20	0.97	0.20
	5	14,076	0.08	88,169	0.09	0.85	0.17

Table 9 continued

Landslide-conditioning factors	Class	Pixels with land slides	Landslide density $\left(\frac{\text{No. of landslide pixels}}{\text{Total landslide pixels}}\right)$	Pixels with non-land slides	Non-landslide density $\left(\frac{\text{No. of pixels in domain}}{\text{Total pixels}}\right)$	$PRL_{i,j}$	Normalised $PRL_{i,j}$
The third principal component	1	16,080	0.09	42,601	0.04	2.00	0.33
	2	45,820	0.26	126,034	0.13	1.93	0.32
	3	66,438	0.37	328,981	0.35	1.07	0.18
	4	44,337	0.25	314,436	0.33	0.75	0.12
	5	6130	0.03	136,465	0.14	0.24	0.04
The fourth principal component	1	14,072	0.08	56,492	0.06	1.32	0.23
	2	27,630	0.15	199,244	0.21	0.74	0.13
	3	42,596	0.24	330,355	0.35	0.68	0.12
	4	58,392	0.33	259,526	0.27	1.19	0.21
	5	36,115	0.20	102,900	0.11	1.86	0.32
Distance from drainage	<50	50,155	0.27	168,335	0.17	1.60	0.34
	50–100	38,145	0.21	159,569	0.16	1.29	0.27
	100–200	47,688	0.26	280,842	0.29	0.91	0.19
	200–500	44,828	0.25	335,772	0.34	0.72	0.15
	>500	1851	0.01	38,125	0.04	0.26	0.05
Lithology	K2	22,166	0.12	121,542	0.14	0.90	0.10
	E1	34,297	0.19	150,630	0.17	1.12	0.13
	E2	65,913	0.36	284,815	0.24	1.49	0.17
	Q1	19,881	0.11	60,452	0.07	1.62	0.18
	E3	17,887	0.10	152,181	0.17	0.58	0.07
	Q2	18,281	0.10	179,066	0.20	0.50	0.06
	Q	3216	0.02	14,522	0.02	1.09	0.12
Distance from roads	<50	9863	0.05	79,428	0.08	0.72	0.16
	50–100	10,558	0.06	100,350	0.09	0.61	0.13
	100–150	28,147	0.15	161,489	0.15	1.01	0.22
	150–200	76,578	0.42	437,252	0.41	1.01	0.22
	>200	57,400	0.31	279,389	0.26	1.19	0.26
Land use	Orchards	17,083	0.09	63,088	0.06	1.46	0.24
	Agriculture	67,782	0.37	433,010	0.44	0.85	0.14
	Forest	83,914	0.46	308,615	0.31	1.47	0.24
	Square	9	0.00	2961	0.00	0.02	0.00
	Urban areas	11,852	0.06	79,860	0.08	0.80	0.13
	Lake	709	0.00	89,474	0.09	0.04	0.01
	River	316	0.00	3795	0.00	0.45	0.07
	Scrublands	0	0.00	860	0.00	0.00	0.00
	Others	1024	0.01	5846	0.01	0.95	0.16

References

- Abay A, Barbieri G (2012) Landslide susceptibility and causative factors evaluation of the landslide area of Debrešina, in the southwestern Afar escarpment, Ethiopia. *J Earth Sci Eng* 2(3):133–144
- Abdi H, Williams LJ (2010) Principal component analysis. *Wiley Interdiscip Rev Comput Stat* 2(4):433–459. doi:[10.1002/wics.101](https://doi.org/10.1002/wics.101)
- Ahmed B (2015) Landslide susceptibility mapping using multi-criteria evaluation techniques in Chittagong Metropolitan Area, Bangladesh. *Landslides* 12(6):1077–1095. doi:[10.1007/s10346-014-0521-x](https://doi.org/10.1007/s10346-014-0521-x)
- Akgun A, Türk N (2010) Landslide susceptibility mapping for Ayvalik (Western Turkey) and its vicinity by multicriteria decision analysis. *Environ Earth Sci* 61(3):595–611. doi:[10.1007/s12665-009-0373-1](https://doi.org/10.1007/s12665-009-0373-1)
- Akgun A, Dag S, Bulut F (2008) Landslide susceptibility mapping for a landslide-prone area (Findikli, NE of Turkey) by likelihood-frequency ratio and weighted linear combination models. *Environ Geol* 54(6):1127–1143. doi:[10.1007/s00254-007-0882-8](https://doi.org/10.1007/s00254-007-0882-8)
- Aleotti P, Chowdhury R (1999) Landslide hazard assessment: summary review and new perspectives. *Bull Eng Geol Environ* 58(1):21–44. doi:[10.1007/s100640050066](https://doi.org/10.1007/s100640050066)
- Ayalew L, Yamagishi H (2005) The application of GIS-based logistic regression for landslide susceptibility mapping in the Kakuda-Yahiko Mountains, Central Japan. *Geomorphology* 65(1):15–31. doi:[10.1016/j.geomorph.2004.06.010](https://doi.org/10.1016/j.geomorph.2004.06.010)
- Ayalew L, Yamagishi H, Ugawa N (2004) Landslide susceptibility mapping using GIS-based weighted linear combination, the case in Tsugawa area of Agano River, Niigata Prefecture, Japan. *Landslides* 1(1):73–81. doi:[10.1007/s10346-003-0006-9](https://doi.org/10.1007/s10346-003-0006-9)
- Ayalew L, Yamagishi H, Marui H, Kanno T (2005) Landslides in Sado Island of Japan: Part II. GIS-based susceptibility mapping with comparisons of results from two methods and verifications. *Eng Geol* 81(4):432–445. doi:[10.1016/j.enggeo.2005.08.004](https://doi.org/10.1016/j.enggeo.2005.08.004)
- Bai SB, Wang J, Lü GN, Zhou PG, Hou SS, Xu SN (2010) GIS-based logistic regression for landslide susceptibility mapping of the Zhongxian segment in the Three Gorges area, China. *Geomorphology* 115(1):23–31
- Ball GH, Hall DJ (1965) Isodata, a novel method of data analysis and pattern classification. Stanford Research Institute, Menlo Park. doi:[10.1016/j.geomorph.2009.09.025](https://doi.org/10.1016/j.geomorph.2009.09.025)
- Borkowski A, Perski Z, Wojciechowski T, Jóźków G, Wójcik A (2011) Landslides mapping in Rożnów Lake vicinity, Poland using airborne laser scanning data. *Acta Geodyn Geomater* 8(3):163
- Bui DT, Lofman O, Revhaug I, Dick O (2011) Landslide susceptibility analysis in the Hoa Binh province of Vietnam using statistical index and logistic regression. *Nat Hazards* 59(3):1413–1444. doi:[10.1007/s11069-011-9844-2](https://doi.org/10.1007/s11069-011-9844-2)
- Bui DT, Tuan TA, Hoang ND, Thanh NQ, Nguyen DB, Van Liem N, Pradhan B (2016) Spatial prediction of rainfall-induced landslides for the Lao Cai area (Vietnam) using a hybrid intelligent approach of least squares support vector machines inference model and artificial bee colony optimization. *Landslides*. doi:[10.1007/s10346-016-0711-9](https://doi.org/10.1007/s10346-016-0711-9)
- Carrara A (1988) Landslide hazard mapping by statistical methods. A black—box approach. In: The proceedings of the workshop on natural disasters in European Mediterranean Countries, Italy, pp 208–224
- Chalkias C, Ferentinou M, Polykretis C (2014) GIS-based landslide susceptibility mapping on the Peloponnese Peninsula, Greece. *Geosciences* 4(3):176–190. doi:[10.3390/geosciences4030176](https://doi.org/10.3390/geosciences4030176)
- Chen W, Li X, Wang Y, Liu S (2013) Landslide susceptibility mapping using LiDAR and DMC data: a case study in the Three Gorges area, China. *Environ Earth Sci* 70(2):673–685. doi:[10.1007/s12665-012-2151-8](https://doi.org/10.1007/s12665-012-2151-8)
- Constantin M, Bednarik M, Jurchescu MC, Vlaicu M (2011) Landslide susceptibility assessment using the bivariate statistical analysis and the index of entropy in the Sibiciu Basin (Romania). *Environ Earth Sci* 63(2):397–406. doi:[10.1007/s12665-010-0724-y](https://doi.org/10.1007/s12665-010-0724-y)
- Dahal RK, Hasegawa S, Nonomura A, Yamanaka M, Masuda T, Nishino K (2008) GIS-based weights-of-evidence modelling of rainfall-induced landslides in small catchments for landslide susceptibility mapping. *Environ Geol* 54:311–324. doi:[10.1007/s00254-007-0818-3](https://doi.org/10.1007/s00254-007-0818-3)
- Dimri S, Lakhera RC, Sati S (2007) Fuzzy-based method for landslide hazard assessment in active seismic zone of Himalaya. *Landslides* 4(2):101–111. doi:[10.1007/s10346-006-0068-6](https://doi.org/10.1007/s10346-006-0068-6)
- Donati L, Turrini MC (2002) An objective method to rank the importance of the factors predisposing to landslides with the GIS methodology: application to an area of the Apennines (Valnerina; Perugia, Italy). *Eng Geol* 63(3):277–289. doi:[10.1016/s0013-7952\(01\)00087-4](https://doi.org/10.1016/s0013-7952(01)00087-4)
- Ermini L, Catani F, Casagli N (2005) Artificial neural networks applied to landslide susceptibility assessment. *Geomorphology* 66(1):327–343. doi:[10.1016/j.geomorph.2004.09.025](https://doi.org/10.1016/j.geomorph.2004.09.025)

- Evans JS, Oakleaf J, Cushman SA, Theobald D (2014) An ArcGIS toolbox for surface gradient and geomorphometric modeling. Version 2.0-0. <http://evansmurphy.wix.com/evansspatial>. Accessed Dec 2015
- Feizizadeh B, Roodposhti MS, Jankowski P, Blaschke T (2014) A GIS-based extended fuzzy multi-criteria evaluation for landslide susceptibility mapping. *Comput Geosci* 73:208–221. doi:[10.1016/j.cageo.2014.08.001](https://doi.org/10.1016/j.cageo.2014.08.001)
- Gessler PE, Moore ID, McKenzie NJ, Ryan PJ (1995) Soil-landscape modelling and spatial prediction of soil attributes. *Int J GIS* 9(4):421–432. doi:[10.1080/02693799508902047](https://doi.org/10.1080/02693799508902047)
- Glenn NF, Streutker DR, Chadwick DJ, Thackray GD, Dorsch SJ (2006) Analysis of LiDAR-derived topographic information for characterizing and differentiating landslide morphology and activity. *Geomorphology* 73(1):131–148. doi:[10.1016/j.geomorph.2005.07.006](https://doi.org/10.1016/j.geomorph.2005.07.006)
- Goetz JN, Brenning A, Petschko H, Leopold P (2015) Evaluating machine learning and statistical prediction techniques for landslide susceptibility modeling. *Comput Geosci* 81:1–11. doi:[10.1016/j.cageo.2015.04.007](https://doi.org/10.1016/j.cageo.2015.04.007)
- Gokceoglu C, Sonmez H, Nefeslioglu HA, Duman TY, Can T (2005) Kuzulu landslide (Sivas, Turkey) and landslide-susceptibility map of its near vicinity. *Eng Geol* 81:65–83. doi:[10.1016/j.enggeo.2005.07.011](https://doi.org/10.1016/j.enggeo.2005.07.011)
- Gorczyca E, Wronska-Walach D, Dlugosz M. (2013) Landslide hazards in the Polish Flysch Carpathians: example of Łososina Dolna Commune. In: *Geomorphological impacts of extreme weather*, Springer, Netherlands, pp 237–250. doi:[10.1007/978-94-007-6301-2_15](https://doi.org/10.1007/978-94-007-6301-2_15)
- Gupta RP, Kanungo DP, Arora MK, Sarkar S (2008) Approaches for comparative evaluation of raster GIS-based landslide susceptibility zonation maps. *Int J Appl Earth Obs Geoinf* 10(3):330–341. doi:[10.1016/j.jag.2008.01.003](https://doi.org/10.1016/j.jag.2008.01.003)
- Guzzetti F, Carrara A, Cardinali M, Reichenbach P (1999) Landslide hazard evaluation: a review of current techniques and their application in a multi-scale study, Central Italy. *Geomorphology* 31(1):181–216. doi:[10.1016/s0169-555x\(99\)00078-1](https://doi.org/10.1016/s0169-555x(99)00078-1)
- Guzzetti F, Mondini AC, Cardinali M, Fiorucci F, Santangelo M, Chang KT (2012) Landslide inventory maps: new tools for an old problem. *Earth Sci Rev* 112(1):42–66. doi:[10.1016/j.earscirev.2012.02.001](https://doi.org/10.1016/j.earscirev.2012.02.001)
- Hengl T, Reuter HI (2009) *Geomorphometry: concepts, software, applications, developments in soil science* 33. Elsevier, Hungary
- Highland L, Bobrowsky PT (2008) *The landslide handbook: a guide to understanding landslides*. US Geological Survey, Reston, p 129. doi:[10.1007/978-3-642-22087-6_5](https://doi.org/10.1007/978-3-642-22087-6_5)
- Jebur MN, Pradhan B, Tehrany MS (2014) Optimization of landslide conditioning factors using very high-resolution airborne laser scanning (LiDAR) data at catchment scale. *Remote Sens Environ* 152:150–165. doi:[10.1016/j.rse.2014.05.013](https://doi.org/10.1016/j.rse.2014.05.013)
- Jenness J, Brost B, Beier P (2011). *Land facet corridor designer: extension for ArcGIS*. Jenness Enterprises. http://www.jennessent.com/downloads/Land_Facet_Tools_A4.pdf. Accessed Dec 2015
- Kanungo DP, Arora MK, Sarkar S, Gupta RP (2006) A comparative study of conventional, ANN black box, fuzzy and combined neural and fuzzy weighting procedures for landslide susceptibility zonation in Darjeeling Himalayas. *Eng Geol* 85(3):347–366. doi:[10.1016/j.enggeo.2006.03.004](https://doi.org/10.1016/j.enggeo.2006.03.004)
- Kanungo DP, Arora MK, Gupta RP, Sarkar S (2008) Landslide risk assessment using concepts of danger pixels and fuzzy set theory in Darjeeling Himalayas. *Landslides* 5(4):407–416. doi:[10.1007/s10346-008-0134-3](https://doi.org/10.1007/s10346-008-0134-3)
- Kavzoglu T, Sahin EK, Colkesen I (2015a) An assessment of multivariate and bivariate approaches in landslide susceptibility mapping: a case study of Duzkoy district. *Nat Hazards* 76(1):471–496. doi:[10.1007/s11069-014-1506-8](https://doi.org/10.1007/s11069-014-1506-8)
- Kavzoglu T, Sahin EK, Colkesen I (2015b) Selecting optimal conditioning factors in shallow translational landslide susceptibility mapping using genetic algorithm. *Eng Geol* 192:101–112. doi:[10.1016/j.enggeo.2015.04.004](https://doi.org/10.1016/j.enggeo.2015.04.004)
- Kayastha P, Dhital MR, De Smedt F (2013) Application of the analytical hierarchy process (AHP) for landslide susceptibility mapping: a case study from the Tinau watershed, west Nepal. *Comput Geosci* 52:398–408. doi:[10.1016/j.cageo.2012.11.003](https://doi.org/10.1016/j.cageo.2012.11.003)
- Kincal C, Akgun A, Koca MY (2009) Landslide susceptibility assessment in the Izmir (West Anatolia, Turkey) city center and its near vicinity by the logistic regression method. *Environ Earth Sci* 59(4):745–756. doi:[10.1007/s12665-009-0070-0](https://doi.org/10.1007/s12665-009-0070-0)
- Kingsbury PA, Hastie WJ, Harrington AJ (1992) Regional landslip hazard assessment using a geographic information system. In *sixth international symposium on landslides*
- Komac M (2012) Regional landslide susceptibility model using the Monte Carlo approach—the case of Slovenia. *Geol Q* 56(1):41–54
- Lee S, Evangelista DG (2006) Earthquake-induced landslide-susceptibility mapping using an artificial neural network. *Nat Hazards Earth Syst Sci* 6(5):687–695. doi:[10.5194/nhess-6-687-2006](https://doi.org/10.5194/nhess-6-687-2006)

- Mahalingam R, Olsen MJ, O'Banion MS (2016) Evaluation of landslide susceptibility mapping techniques using lidar-derived conditioning factors (Oregon case study). *Geomat Nat Hazards Risk*. doi:[10.1080/19475705.2016.1172520](https://doi.org/10.1080/19475705.2016.1172520)
- Mashari S, Solaimani K, Omidvar E (2012) Landslide susceptibility mapping using multiple regression and GIS tools in Tajan Basin, North of Iran. *Environ Nat Resour Res* 2(3):43. doi:[10.5539/enrr.v2n3p43](https://doi.org/10.5539/enrr.v2n3p43)
- McKean J, Roering J (2004) Objective landslide detection and surface morphology mapping using high-resolution airborne laser altimetry. *Geomorphology* 57(3):331–351. doi:[10.1016/s0169-555x\(03\)00164-8](https://doi.org/10.1016/s0169-555x(03)00164-8)
- Mezughhi TH, Akhir JM, Rafek AGM, Abdullah I (2011) Landslide susceptibility assessment using frequency ratio model applied to an area along the EW highway (Gerik-Jeli). *Am J Environ Sci* 7(1):43–50
- Mohammady M, Pourghasemi HR, Pradhan B (2012) Landslide susceptibility mapping at Golestan Province, Iran: a comparison between frequency ratio, Dempster-Shafer, and weights-of-evidence models. *J Asian Earth Sci* 61:221–236. doi:[10.1016/j.jseae.2012.10.005](https://doi.org/10.1016/j.jseae.2012.10.005)
- Moore ID, Grayson RB, Ladson AR (1991) Digital terrain modelling: a review of hydrological, geomorphological, and biological applications. *Hydrol Process* 5:3–30. doi:[10.1002/hyp.3360050103](https://doi.org/10.1002/hyp.3360050103)
- Moore ID, Gessler PE, Nielsen GA, Petersen GA (1993) Terrain attributes: estimation methods and scale effects. In: Jakeman AJ, Beck MB, McAleer M (eds) *Modeling change in environmental systems*. Wiley, London, pp 189–214
- Ozturk U, Tarakegn YA, Longoni L, Brambilla D, Papini M, Jensen J (2016) A simplified early-warning system for imminent landslide prediction based on failure index fragility curves developed through numerical analysis. *Geomat Nat Hazards Risk* 7(4):1406–1425. doi:[10.1080/19475705.2015.1058863](https://doi.org/10.1080/19475705.2015.1058863)
- Pawluszek K, Borkowski A (2016) Landslides identification using Airborne Laser Scanning data derived topographic terrain attributes and support vector machine classification. *The International Archives of the Photogrammetry, Remote Sensing and Spatial Information Sciences - XXIII ISPRS Congress, Prague, Czech Republic, 12–19 July 2016, Vol. XLI-B8 No. Comm. VIII, WG VIII/1, Göttingen, Germany, pp 145–149*. doi:[10.5194/isprs-archives-XLI-B8-145-2016](https://doi.org/10.5194/isprs-archives-XLI-B8-145-2016)
- Pawluszek K, Ziaja M, Borkowski A (2014) Accuracy assessment of the height component of the airborne laser scanning data collected in the ISOK system for the Widawa River Valley. *Acta Sci Pol Geod Descr Terr* 13(3–4):27–38
- Pourghasemi HR, Mohammady M, Pradhan B (2012) Landslide susceptibility mapping using index of entropy and conditional probability models in GIS: Safarood Basin, Iran. *Catena* 97:71–84. doi:[10.1016/j.catena.2012.05.005](https://doi.org/10.1016/j.catena.2012.05.005)
- Pourghasemi HR, Pradhan B, Gokceoglu C, Mohammadi M, Moradi HR (2013) Application of weights-of-evidence and certainty factor models and their comparison in landslide susceptibility mapping at Haraz watershed, Iran. *Arab J Geosci* 6(7):2351–2365. doi:[10.1007/s12517-012-0532-7](https://doi.org/10.1007/s12517-012-0532-7)
- Pourghasemi HR, Moradi HR, Aghda SF, Gokceoglu C, Pradhan B (2014) GIS-based landslide susceptibility mapping with probabilistic likelihood ratio and spatial multi-criteria evaluation models (North of Tehran, Iran). *Arab J Geosci* 7(5):1857–1878. doi:[10.1007/s12517-012-0825-x](https://doi.org/10.1007/s12517-012-0825-x)
- Remondo J, González A, De Terán JRD, Cendrero A, Fabbri A, Chung CJF (2003) Validation of landslide susceptibility maps; examples and applications from a case study in Northern Spain. *Nat Hazards* 30(3):437–449. doi:[10.1023/b:nhaz.0000007201.80743.fc](https://doi.org/10.1023/b:nhaz.0000007201.80743.fc)
- Rivest JF, Soille P, Beucher S (1992) Morphological gradients. In *SPIE/IS&T 1992 symposium on electronic imaging: science and technology*. International Society for Optics and Photonics, pp 139–150. doi: [10.1117/12.58373](https://doi.org/10.1117/12.58373)
- Saadatkah N, Azman K, Lee ML (2014) Qualitative and quantitative landslide susceptibility assessments in Hulu Kelang area, Malaysia. *EJGE C* 19(2014):545–563. doi:[10.1007/s10706-014-9818-8](https://doi.org/10.1007/s10706-014-9818-8)
- Saaty TL (1977) A scaling method for priorities in hierarchical structures. *J Math Psychol* 15(3):234–281. doi:[10.1016/0022-2496\(77\)90033-5](https://doi.org/10.1016/0022-2496(77)90033-5)
- Saaty TL (1980) *The analytic hierarchy process: planning, priority setting, resources allocation*. McGraw, New York
- Saaty TL (2000) *Fundamentals of decision making and priority theory with the analytic hierarchy process*, vol 6. Rws Publications, Pittsburgh. doi:[10.1007/978-94-015-9799-9_2](https://doi.org/10.1007/978-94-015-9799-9_2)
- Sarkar S, Kanungo DP (2004) An integrated approach for landslide susceptibility mapping using remote sensing and GIS. *Photogramm Eng Remote Sens* 70(5):617–625. doi:[10.14358/pers.70.5.617](https://doi.org/10.14358/pers.70.5.617)
- Schulz WH (2004) *Landslides mapped using LIDAR imagery, seattle, Washington*. U.S. Geological Survey Open-File Report 2004-1396
- Schuster RL, Fleming RW (1986) Economic losses and fatalities due to landslides. *Bull As Eng Geol* 23(1):11–28. doi:[10.2113/gseegeosci.xxiii.1.11](https://doi.org/10.2113/gseegeosci.xxiii.1.11)
- Soille P (2013) *Morphological image analysis: principles and applications*. Springer, Berlin

- Solanas Pérez A, Manolov R, Leiva Ureña D, Richard's MM (2011) Retaining principal components for discrete variables. *Anu Psicol* 41(1–3):33–50
- Starkel L (1972) An outline of the relief of the Polish Carpathians and its importance for human management. *Probl Zagospod Ziem Gór* 10:75–150
- Stüzen ML, Doyuran V (2004) A comparison of the GIS based landslide susceptibility assessment methods: multivariate versus bivariate. *Environ Geol* 45(5):665–679. doi:[10.1007/s00254-003-0917-8](https://doi.org/10.1007/s00254-003-0917-8)
- Thiery Y, Malet JP, Sterlacchini S, Puissant A, Maquaire O (2007) Landslide susceptibility assessment by bivariate methods at large scales: application to a complex mountainous environment. *Geomorphology* 92(1):38–59. doi:[10.1016/j.geomorph.2007.02.020](https://doi.org/10.1016/j.geomorph.2007.02.020)
- Van Den Eeckhaut M, Poesen J, Verstraeten G, Vanacker V, Moeyersons J, Nyssen J, van Beek LPH, Vandekerckhove L (2007) Use of LIDAR-derived images for mapping old landslides under forest. *Earth Surf Proc Land* 32:754–769. doi:[10.1002/esp.1417](https://doi.org/10.1002/esp.1417)
- van Westen CJ, Castellanos E, Kuriakose SL (2008) Spatial data for landslide susceptibility, hazard, and vulnerability assessment: an overview. *Eng Geol* 102(3):112–131. doi:[10.1016/j.enggeo.2008.03.010](https://doi.org/10.1016/j.enggeo.2008.03.010)
- Wilson JP, Gallant JC (2000) *Terrain analysis principles and applications*. Wiley and Sons, New York
- Woźniak A (2014) Anomalously high monthly precipitation totals in the Polish Carpathian Mountains and their foreland (1881–2010). *Prace Geograficzne*. 138:7–28 **[in Polish]**
- Yalcin A, Reis S, Aydinoglu AC, Yomralioglu T (2011) A GIS-based comparative study of frequency ratio, analytical hierarchy process, bivariate statistics and logistics regression methods for landslide susceptibility mapping in Trabzon, NE Turkey. *Catena* 85(3):274–287. doi:[10.1016/j.catena.2011.01.014](https://doi.org/10.1016/j.catena.2011.01.014)